NASA Technical Memorandum 80223

NASA-TM-80223 19800009757

FLIGHT PERFORMANCE OF THE TCV B-737 AIRPLANE AT JORGE NEWBERY AIRPORT, BUENOS AIRES, ARGENTINA USING TRSB/MLS GUIDANCE

WILLIAM F. WHITE AND LEONARD V. CLARK

JANUARY 1980

NASA
National Aeronautics and Space Administration

Langley Research Center
Hampton, Virginia 23665

SUMMARY

On October 27, through November 4, 1977, the Terminal Configured Vehicle (TCV) B-737 airplane was flown at Jorge Newbery Airport in Buenos Aires, Argentina in support of the Federal Aviation Administration (FAA) demonstration of the U. S. candidate Time Reference Scanning Beam (TRSB) Microwave Landing System (MLS).

The objective of the National Aeronautics and Space Administration (NASA) participation in the TRSB/MLS demonstration program was to demonstrate practical utilization of MLS guidance for curved, noise abatement approaches and at the same time acquire useful pilot operational experience. The formal demonstration flights at Jorge Newbery consisted of 53 automatic approaches. The demonstration flights were preceded by other manual and automatic checkout flights to verify the acceptability of the processed MLS parameters, and to evaluate the performance of the airplane along several candidate curved-path approaches. On the basis of results from these checkout flights the two shortest approaches were selected for demonstration. The report presents a summary of the flight performance of the TCV airplane during the demonstration automatic approaches and landings while utilizing TRSB/MLS guidance. Detailed analyses of the performance data are not presented herein.

INTRODUCTION

The NASA Langley Research Center's Terminal Configured Vehicle (TCV) program operates a highly modified Boeing 737 airplane which contains a second research cockpit in addition to a large amount of experimental navigation, guidance, and control equipment for conducting flight research on advanced avionics systems and displays. The FAA requested that NASA use the TCV B-737 to provide demonstrations of the TRSB/MLS being proposed by the United States as a new international standard landing guidance system to replace the presently used Instrument Landing System (ILS) and Precision Approach Radar (PAR). The first such demonstration was conducted at the FAA's National Aviation Facilities Experimental Center (NAFEC) at Atlantic City, New Jersey in May 1976 for members of the International Civil Aviation Organization (ICAO), industry and government officials, and representatives of the news media. The flight results from the NAFEC demonstration are documented in references 1 and 2 which also include descriptions of the TCV airplane equipment, MLS processing, and control laws. The latter were modifications of the original RNAV and ILS autoland control laws, since insufficient time was

available to develop new control laws designed for curved paths using MLS. Similar demonstrations were subsequently requested for Buenos Aires, Argentina in October 1977, for New York in December 1977, and for Montreal, Canada in March 1978.

This report summarizes the flight performance results of the TCV airplane during the demonstration automatic approaches and landings conducted at the Jorge Newbery Airport in Buenos Aires, Argentina. The TRSB system demonstrated at Jorge Newbery was installed on runway 13 and consisted of the Basic Narrow azimuth and elevation subsystems and a precision L-band DME (reference 3). Observers carried on these demonstration flights were primarily attendees of a meeting of the Organization of American States Aeronautical Telecommunications Group, representing 19 countries. Reference 4 is a magazine article describing the MLS demonstration flights at Jorge Newbery. For comparison purposes reference 5 describes the flight performance of the TCV B-737 while utilizing TRSB/MLS guidance at JFK airport, which was conducted about one month after the flights at Jorge Newbery Airport.

ABBREVIATIONS AND SYMBOLS

AZ	Microwave Landing System azimuth guidance
CAT I	Category I Landing Minima {71 m (200 ft) decision height, 732 m (2400 ft) runway visual range}
CAT II	Category II Landing Minima {30.5m (100ft) decision height, 366m (1200ft) runway visual range}
CWS	Control Wheel Steering
DELTH	Vertical error signal input to autoland control law
DELTY	Lateral error signal input to autoland control law (negative of cross track error)
DH	Decision Height
DME	Distance Measurement Equipment
EADI	Electronic Attitude Director Indicator
EHSI	Electronic Horizontal Situation Indicator
EL	Microwave Landing System elevation guidance
FAF	Final Approach Fix

GPIP	Glide Path Intercept Point
h_{MLS}	Altitude above sea level derived from Microwave Landing System
h_R	Radio altitude
$\dot{h}_{CF}$	Complementary-filtered barometric vertical speed
$\dot{h}_{MLS}$	Vertical speed derived from Microwave Landing System
HER	Vertical error signal input to RNAV control law (negative of altitude error)
IDD	Inertial and dual DME area navigation mode
IDDALT	Inertially quickened barometric altitude above sea level
IDX	Inertial and single DME area navigation mode
ILS	Instrument Landing System
IMC	Instrument Meteorological Conditions
INS	Inertial Navigation System
IXX	Inertial area navigation mode
MLS	Microwave Landing System
MSL	Mean sea level
NAFEC	National Aviation Facilities Experimental Center
NCDU	Navigation Control and Display Unit
NCU	Navigation Computer Unit
PAR	Precision Approach Radar
PDME	Precision DME
RNAV	Area navigation
R_{Rhumb}	Rhumb line distance from GPIP (60 X Δ latitude ÷ cosine of the course angle from true North)

SID	Standard Instrument Departure
STAR	Standard Terminal Arrival Route
TRSB	Time Reference Scanning Beam
VOR	Very high frequency Omnidirectional Range
$\hat{X}$	Estimated distance along runway centerline extended from MLS azimuth antenna
XTK	Lateral error signal input to RNAV control law
$\hat{Y}$	Estimated perpendicular distance from runway centerline extended
Δh	Height above GPIP
ΔH	Vertical distance from glide path
ΔHER	Change in HER at conventional-to-MLS RNAV transition
ΔXTK	Change in XTK at conventional-to-MLS RNAV transition
Δy	Perpendicular distance from runway centerline

TCV RESEARCH AIRPLANE

The TCV Program operates a Boeing 737-100 airplane (Figure 1) to conduct flight research aspects of the program. The airplane is equipped with a special research flight deck, located about 6m (20 ft) aft of the standard flight deck. An extensive array of electronic equipment and data recording systems is installed throughout the former passenger cabin (Figure 2).

The airplane can be flown from the aft flight deck using advanced electronic displays and semi-automatic or automatic control systems that can be programmed for research purposes. Two safety pilots located in the front flight deck are responsible for all phases of flight safety and most traffic clearances. Two research pilots usually fly the airplane from the aft cockpit during test periods, which can last from take-off through landing. The only normal flight systems that cannot be controlled from the aft flight deck are the landing gear and the speed brakes, which are operated by the safety pilots in response to annunciators. The safety pilots can take control of the airplane at any time by over-powering the aft flight deck controls or by disengaging the aft flight deck.

The aft flight deck (Figure 3) includes three monochromatic Cathode Ray Tube (CRT) displays that are available to each research pilot. The lower display is the Navigation Control and Display Unit (NCDU) which allows each pilot to control and monitor the airplane's navigation computer. The computer can access airway, Standard Instrument Departure (SID), Standard Terminal Arrival Route (STAR), and runway data for the geographic area of interest.

The center display is an Electronic Horizontal Situation Indicator (EHSI) that provides each pilot with a pictorial navigation display of the airplane's position relative to desired guidance path, flight plan waypoints, and selectable local points of interest such as airfields, obstructions and radio navigation aids.

The top display is an Electronic Attitude Director Indicator (EADI) that provides the pilots with a display of the airplane's pitch and roll attitude for instrument flight. Other symbols for flight path acceleration, flight path angle (actual and commanded), lateral and vertical guidance, and speed error are integrated into the EADI display format. A forward-looking television image (from a TV camera located in the airplane's nose) can be presented on the EADI in registration with the symbols. Based on navigation position estimates a computer-generated runway drawing, showing the true perspective of the runway, can also be displayed during approach and landing.

The TCV airplane's navigation, autoland and autothrottle systems permit the plane to fly complex two-, three-, and four-dimensional (position and time control) flight paths. The flight plan can either be programmed before take-off or developed and modified in flight through the navigation computer's keyboard. An on-board data acquisition system records pertinent flight information for analysis after a test. Information can also be transmitted to a ground station within a range of 50 n. mi.

MLS APPROACHES INTO JORGE NEWBERY

The approach paths flown at Jorge Newbery Airport utilizing TRSB/MLS guidance are shown in figure 4 superposed on a map of the area. These MLS approach paths were selected to reduce the noise impact compared with conventional long straight-in ILS approaches which overfly heavily populated residential areas. The MLS approaches were entirely over the river until the end of the final turn. Jorge Newbery Airport has a single runway located about four km from downtown Buenos Aires. It handles a high volume of short haul and commuter traffic.

The MLS configuration the FAA chose for the Jorge Newbery Airport installation was the Basic Narrow (aperture) with ± 40 degrees azimuth coverage. This equipment was located on runway 13 as shown in figure 5.

The two approach patterns (STARs) chosen for the test/demonstration, ABE04 and ABE05, are shown in some detail in figures 6, 7, and 8. Both patterns began at an altitude of 914m (3000 ft) over the river at 5 to 6 n. mi. laterally from the runway. A constant 3-degree descent began at the initial waypoint of each approach. ABE04 required a 90-degree turn into a three km (1.6 n. mi.) straight final whereas ABE05 required a 60-degree turn into a two km (1.1 n. mi.) final. Both approaches took a little over three minutes to complete from the initial waypoint. The control law schedule of the TCV B-737 during the automatic approaches and landings is depicted in figure 9.

FLIGHT RESULTS AND DISCUSSION

Flight performance data obtained during the TRSB/MLS demonstration flights of the TCV B-737 at Jorge Newbery are presented in table 1. These data are presented in chronological order for selected points along the approach and landing path: At conventional-to-MLS RNAV transition, the final approach fix, the CAT I decision height, at decrab, the CAT II decision height, at flare initiation, and at touchdown. The final approach fix data are shown as determined from both the navigation and flight control computers. At this point the lateral axis was still being controlled by the RNAV system, and the longitudinal axis was in the autoland glide path tracking mode. The data therefore represent flight technical error of the RNAV system in the lateral axis, and of the autoland system in the longitudinal axis. Forty-three ABE04 approaches were flown and ten ABE05 approaches. Fifty-two of the these approaches resulted in automatic landings, although the data indicated that safety pilot intervention occurred in four of these just prior to touchdown. A safety pilot take over and go-around at low altitude was caused during one of the approaches by a previous landing aircraft which had not cleared the runway.

Wind Conditions

Wind speed and direction versus altitude was obtained from the navigation computer estimates. The mean horizontal components in the north-referenced system were calculated for selected altitudes, along with the dispersions. The mean component speeds were then used to calculate a prevailing wind for each altitude. The north and east components and the resultant winds are presented in table II for altitudes from 15m (50 ft) to 305m (1000 ft) above sea level.

Unlike some other B-737 MLS demonstrations, in this case unfavorable winds were not routinely experienced. Table II shows that the mean wind at flare initiation was a five knot direct head wind. On flights 193A and 193B winds in excess of 40 knots were encountered less than 305m (1000 ft) from the ground, but at no time were cross wind components greater than ten knots or tail wind components greater than five knots measured during flare and landing.

Typical Approach Data

Representative data for one of the approaches are presented in figure 10 showing the cross track and altitude deviations from the planned curved approach path according to the received MLS signals. These data do not indicate performance of the MLS, but rather performance of the airplane's guidance system utilizing MLS. However, analysis of photo-theodolite tracking data from reference 1 indicates that the MLS guidance accuracy is comparable to the photo-theodolite tracker accuracy, and therefore the MLS-derived position errors may be considered a good indication of path following error magnitudes. Further evidence may be seen in figure 11, which presents ground tracking data from one of the Buenos Aires data runs. A manually operated radio telemetering theodolite was used for azimuth tracking and an Australian optical television tracker for elevation (reference 3). The azimuth angle errors translate into maximum cross track errors of about two meters except for the two spikes of about four meters near waypoint FAF3K. The elevation errors correspond to altitude errors of somewhat less than five meters at waypoint FAF3K and two meters at the CAT I decision height. The aircraft guidance signals would be expected to show somewhat less error due to the use of alpha-beta filtering on the MLS signals, and complementary filtering on the aircraft's estimated position coordinates (reference 2).

The plots in figure 10 are annotated to indicate various discrete events along the approach according to the control law schedule shown in figure 9. At TRSB enable the airplane guidance changes from conventional RNAV (IDD/IDX/IXX) to MLS RNAV. During its constant 3-degree curved descent the airplane approaches the final 3-degree planar glide path from above. The switch from RNAV to autoland vertical guidance occurs when the airplane comes within 0.108 degrees of the planar glide path. The switch from RNAV to autoland guidance in the lateral axis occurs shortly past the final approach fix, when the aircraft rolls out to less than a 3-degree bank angle, with a ground track angle within 0.27 degrees of runway heading and an azimuth angle error of not over 0.2 degrees from runway centerline. Decrab occurs at an altitude of 45.7m (150 ft) provided lateral guidance is in the autoland mode. Flare initiation occurs at variable altitude depending on the airplane's sink rate.

The variables XTK and the negative of HER represent flight technical errors for the lateral and longitudinal axes of the autopilot when in RNAV control mode, respectively. In the autoland control mode, the corresponding errors are DELTY and DELTH. For this demonstration, the error due to limiting of the magnitude of the errors being input to the control laws. This limiting was a feature of the original ILS autoland control laws to prevent excessive aircraft maneuvering at low altitudes. It became a problem only when attempting these very short final approaches. Figure 12 illustrates the problem which sometimes occurred: the limited value of DELTY at the final approach fix was about -15m, but the MLS-derived position error Δy was over twice that value (table I). The limiting reduced control law response to the point that DELTY remained at the limit value until almost over threshold, resulting in poorer runway centerline tracking than should have been the case. DELTY in this case is not a valid indication of path following or of guidance errors. The values of cross track error Δy given in table I were obtained from the position estimate $\hat{y}$, rather than DELTY.

The situation does not appear as critical for DELTH in figure 12. However, the limit does reduce to about 1m at the threshold, so that limiting of the guidance error signal does occur more and more frequently as range is reduced. In the longitudinal case, it was normal for the limit to be reached only occasionally and briefly as seen in figure 12, rather than continually as shown for DELTY. Nevertheless, these occasional encounters with the DELTH limits contribute somewhat to increased touchdown dispersion due to the reduced sensitivity to large glide path tracking errors. Subsequent to the Jorge Newbery demonstrations, performance was improved by allowing the limits to decrease with range only down to a minimum value of ±9.7m (31.9 ft) for DELTY and ±4.6m (15 ft) for DELTH.

Conventional-to-MLS RNAV Transition Offsets

Figure 13 and 14 present a summary of the TRSB-derived position estimates $\hat{x}$ and $\hat{y}$ at the time of TCV B-737 airplane transition from conventional RNAV guidance for each approach path. The location of this transition point was dependent first upon the reception of valid MLS azimuth, elevation and precision range data being received for 10 seconds; and a subsequent pilot-initiated switch at his discretion after receiving the MLS valid annunciation. Not all of the approaches appear on these figures since the data reduction started after the transition for some approaches.

Figure 15 summarizes conventional-to-MLS RNAV transition data for the approaches shown in figures 13 and 14. The numbers represent the change in XTK and HER (flight technical error) upon switching to MLS guidance. The mean values of ΔXTK = 21.4m and -ΔHER = 0.6m indicate that the aircraft was typically slightly to the right of the intended horizontal track, and almost exactly on the intended vertical path. The largest horizontal path offset observed during the demonstration flights was -529m, and the largest altitude offset was 106m.

During the initial checkout flights, RNAV accuracy problems were experienced due to the availability of only a single DME (Ezeiza) within range. The first two runs had cross track offsets of -604m and -185m, which caused late reception of valid MLS signals and adversely affected performance. An attempt was made to operate with pure inertial navigation, but the time lapse between INS initialization and the completion of the flight allowed INS drift to cause errors up to 1053m. The problem was reduced by adding the location and frequency of the MLS Precision DME to the navigation computer bulk data and using it as a conventional navaid in the RNAV mode. The PDME did not have an omnidirectional antenna, but provided enough coverage to prevent consistently large negative cross track errors.

Automatic Approach and Landing Criteria

Figure 16 schematically depicts the FAA certification criteria for approaches and automatic landings using ILS guidance (and some points used for data analysis). The flight performance data from table I are compared with these criteria in figures 17 to 23 in order to provide some quantitative aspect of the TCV B-737 approach and landing performance utilizing MLS guidance in lieu of conventional ILS guidance.

Final Approach Fix Delivery Errors. Figures 17 and 18 present the autopilot guidance errors at the final approach fix as determined from the navigation and flight control computers, respectively. At this point the cross track flight technical error is represented by XTK (figure 17), since localizer mode engage has not yet occurred, and vertical flight technical error is given by ΔH (figure 18). At this point the navigation and flight control computers agreed to 0.1m on the mean autopilot error in the vertical direction. The 24.6m difference between the lateral errors is due in part to an attempt to improve RNAV system delivery accuracy. Figure 17 indicates a tendency of the RNAV system to develop

a standoff guidance error in turns, resulting in an overshoot of the runway centerline when turning final approach. After inflight estimates of error were made on the first few approaches, an attempt was made to cancel the overshoot error by moving the final approach waypoint location off centerline. Unfortunately, these approaches were not typical of performance during the demonstration flights. As can be seen from figure 18, the correction was approximately double that needed, with the result that the aircraft consistently undershot the centerline.

Localizer and Glide Path Tracking Errors. Figures 19 through 22 show the MLS-derived position errors at the CAT I decision height, decrab initiation, the CAT II decision height, and at flare initiation, respectively. These are not necessarily indicative of flight technical errors due to the artificial limiting of the guidance error signals in some cases. An illustration of the effect of this limiting is seen in the point at the far left in figure 19, and the slowness with which this large error is being corrected (figures 20 and 21). A similar case for altitude is seen in the point indicating an approach where the aircraft is over 5m below glide path at the CAT I decision height, is slowly correcting, and then begins to run into limited error signals so that the glide path error is still almost -7m at flare initiation.

Touchdown Performance. Several methods of determining touchdown time were investigated. The first involved data discretes from the autopilot data formatter, which gave the time at which the squat switch closed and when one of the main gear wheels spun up to approximately 60 knots. This data was available at a sampling rate of 20/second. The second method involved the time history plotting on an expanded scale of vertical acceleration and left outboard wheel speed (the right wheel sensor was inoperative). The time of touchdown was fixed as being the time at which a positive increase was seen on either of these variables. The sampling rate for this data was 40/second, and the two were sampled at different times in each data frame. A comparison of the techniques showed that touchdown time as determined from the data formatter discretes occurred 0.20 ± 0.13 seconds later than that obtained from vertical acceleration, and 0.18 ±0.12 seconds later than that from the outboard wheel speed. For this study touchdown time was taken from vertical acceleration or wheel speed, whichever gave the first indication.

Touchdown position was determined from the MLS-derived estimates of latitude and longitude, from which a rhumb-line calculation of distance past the GPIP was made. On four of the landings the data indicated significant control inputs by the safety pilot in the form of control column back pressure. It is uncertain how this affected the dispersion statistics since on two of those landings the aircraft had floated well past the mean touchdown point, and the landings were among the longest already without further delaying touchdown. However, these landings may have had slightly lower sink rates at touchdown than would otherwise have been the case. Statistics are given in table I for all 52 landings and for the 48 "unassisted" ones.

Touchdown sink rate was determined from the MLS-derived vertical speed. Table III compares MLS and complementary-filtered barometrically derived sink rates at several points along the path. Agreement is generally good, with a small systematic difference which appears to correlate with the MLS elevation error in figure 11. However, there is a much larger difference at touchdown, due to errors induced in barometric quantities by ground effect. Although touchdown occurs well past the MLS elevation coverage zone, the MLS-derived quantities are still accurate because radio altitude is substituted when MLS elevation coverage is lost. The ground effect may also be seen in the change in barometric altitude error in table IV. The 3m drop in error during the last 30m of descent is not consistent with the error trend developed earlier on the approach, or with the other methods of altitude measurement.

Comparison of MLS Altitude With Other Altitude Measurements

The indicated altitude error of the aircraft at several points between the final approach fix and touchdown was calculated using MLS, radio, and inertially-quickened barometric altitude indications. The estimated position $\hat{X}$ was used to determine the desired altitude above sea level at each point. In the case of the radio altimeter, the altitude above ground and above sea level were identical at the final approach fix for most of the approaches. At the intermediate points, it was assumed that the ground level was the same as the glide path intercept point altitude. This assumption contributed an unknown error since the ground was not perfectly flat.

The data of table IV represent flight technical error as determined by several data sources. The radio altitude data at the intermediate points is subject to uncertainty due to the unknown terrain profile. Note that the radio and MLS altitudes are repeatable to within approximately 0.5m, as compared to nearly 17m for the barometrically-derived altitude; and that the radio (over known terrain) and MLS altitudes did not exhibit the large bias and ground effect perturbations shown by the barometric altitude.

CONCLUDING REMARKS

The Buenos Aires TRSB/MLS demonstration presented in many ways much more of a challenge than the original ICAO MLS demonstration at NAFEC in Atlantic City, New Jersey. The final approaches were much shorter, and the TRSB system demonstrated provided only $\pm 40^{\circ}$ coverage in azimuth, as compared to the $\pm 60^{\circ}$ of the original test bed system. This allowed for considerably less time of operation within the MLS coverage region prior to attempting an autoland, a problem which was compounded by the scarcity of navigation aids in the Buenos Aires vicinity as compared to Atlantic City. Further, performance was hurt to some extent by guidance error signal limiting at close ranges, a problem which did not occur previously since the 3 n.mi. final approach at NAFEC allowed sufficient time to stabilize on the final approach before encountering such small error limit bands. In spite of these problems, the data for 52 approaches and landings were within the FAA certification criteria for CAT II approaches and for autoland systems. MLS-derived altitude was shown to be equivalent to that which was attained by radio altitude but without the terrain dependency, and superior to barometric altitude in both accuracy and repeatability. The capability to automatically fly curved, noise-abatement type approaches and landings with final legs as short as 2km (1.1 n.mi.) was demonstrated.

REFERENCES

1. Paulson, C. V. and Weener, E. F.: The TCV B-737 Flight Performance During the Demonstration of the Time Reference Scanning Beam Microwave Landing System to the International Civil Aviation Organization All Weather Operations Panel. Boeing Commercial Airplane Company Document No. D6-44291, February 1977.

2. White, William F., et al.: Flight Demonstrations of Curved, Descending Approaches and Automatic Landings Using Time Reference Scanning Beam Guidance. NASA Technical Memorandum 78745, May 1978.

3. Anon: TRSB Microwave Landing System Demonstration Program at Jorge Newbery Aeroparque, Buenos Aires, Argentina. FAA Report No. FAA-RD-78-14, 1978.

4. Anon: MLS demonstrated in Argentina, Aviation Week and Space Technology, November 14, 1977, p. 23.

5. White, William F. and Clark, Leonard V.: Flight Performance of the TCV B-737 Airplane at Kennedy Airport Using TRSB/MLS Guidance. NASA Technical Memorandum 80148, July 1979.

6. FAA Advisory Circular No. 120-29: Criteria for Approving Category I and Category II Landing Minima for FAR 121 Operations, September 1970.

7. FAA Advisory Circular No. 120-28B: Criteria for Approval of Category IIIa Landing Weather Minima, December 1977.

8. FAA Advisory Circular No. 20-57A: Automatic Landing Systems, January 1971.

TABLE I. - SUMMARY OF FLIGHT PERFORMANCE OF THE TCV B-737 AT JORGE NEWBERY AIRPORT USING TRSB-MLS GUIDANCE

DATE	FLT/RUN	CONVENTIONAL-TO-MLS RNAV TRANSITION (ref. figures 13, 14 and 15)			FINAL APPROACH FIX (ref. figure 17)		FINAL APPROACH FIX (ref. figure 18)		CAT I DECISION HEIGHT (ref. figure 19)	
		$\hat{Y}$, m *1	ΔXTK, m *2	-ΔHER, m *2	XTK, m *2	-HER, m *2	Δy, m *1	ΔH, m *1	Δy, m *1	ΔH, m *1
10/27/77	190-3R2	- 4098.6	-48.8	6.1	24.3	4.9	---	4.0	-4.8	-1.3
	190-4	- 5085.6	243.8	-8.5	4.1	2.7	8.8	3.0	-6.1	-2.4
10/28/77	191-2R1	- 4211.1	-309.7	106.1	33.8	2.0	8.6	1.5	-4.1	-0.9
	191-3	- 5808.0	12.2	50.0	8.2	1.2	9.4	1.0	-3.5	-1.5
	191-4	- 4099.3	61.0	7.3	1.3	3.7	-26.4	3.5	2.5	1.2
	191-5	- 5572.4	36.6	80.5	9.4	3.7	9.9	3.5	-3.7	-1.6
10/29/77	192-3	- 4354.1	252.4	52.4	22.0	5.2	-4.8	4.6	-2.1	-1.0
	192-4	- 5189.8	309.7	13.4	-7.0	3.7	-32.3	4.0	-20.1	-2.6
	192-3R1	- 3794.5	-17.1	19.5	7.9	3.7	-15.7	3.7	1.0	0.8
	192-4R1	- 4679.3	-17.1	12.2	14.1	5.0	-11.6	5.5	-1.3	-3.2
10/31/77	193A-3	(5)	(5)	(5)	5.1	2.4	-20.5	2.1	0.1	1.0
	193A-3R1	- 2246.1	-154.8	-8.5	-3.6	1.2	-28.3	0.9	0.7	-1.0
	193A-3R2	(5)	(5)	(5)	3.2	2.4	-21.9	2.0	-0.9	-2.7
	193A-3R3	- 3136.1	-139.0	- 9.8	11.9	1.2	-14.2	1.2	1.0	1.6
	193B-3	- 4166.6	-167.0	18.3	9.7	1.2	-14.3	0.5	-2.6	0.1
	193B-3R1	(5)	(5)	(5)	2.4	1.2	(4)	1.2	-0.7	1.8
	193B-3R2	- 3671.3	-201.2	23.2	-9.9	1.2	-35.4	1.2	0.2	2.1
	193B-3R3	(5)	(5)	(5)	25.3	0	-2.2	0.1	-4.1	1.2
	193B-5	(5)	(5)	(5)	31.2	0	3.4	0.4	-4.9	-2.3
11/1/77	194A-3	- 4269.0	398.7	6.1	21.8	2.4	-3.0	2.5	-1.3	1.1
	194A-3R1	(5)	(5)	(5)	8.5	3.7	-17.5	3.4	2.2	-0.3
	194A-3R2	- 4463.8	367.0	41.5	11.7	3.7	-16.0	3.0	2.1	0.2
	194A-3R3	(5)	(5)	(5)	5.7	4.9	-19.3	4.4	-0.9	0.3
	194A-3R4	(5)	(5)	(5)	14.7	2.4	-13.4	2.1	-1.0	1.1
	194A-XYZ	(5)	(5)	(5)	2.3	6.1	-22.8	5.2	-3.6	-1.0
	194B-4	(5)	(5)	(5)	25.3	2.4	0	1.9	-3.2	-0.7
	194B-5	- 3793.8	-529.1	- 8.5	27.6	3.7	3.5	3.8	1.3	-1.5
	194C-4R1	- 3688.7	112.2	- 32.9	9.4	2.4	-16.6	1.7	0.8	3.0
	194C-5	- 3717.0	-18.3	- 22.0	12.2	1.2	-14.7	0.9	0.5	0.1
11/2/77	195A-4	- 4041.6	187.8	- 13.4	5.0	4.0	-20.9	4.3	0.2	-0.5
	195A-4R1	- 4244.9	206.0	- 8.5	6.1	4.9	-20.2	5.1	0.7	-5.5
	195A-5	- 4250.7	51.2	- 8.5	5.1	5.4	-30.7	5.2	2.6	2.3
	195B-4	- 4177.0	588.9	- 9.8	6.1	4.9	-20.2	5.2	2.9	-1.0
	195B-4R1	- 4170.0	285.3	-11.0	17.5	7.3	-9.8	6.7	3.7	-2.9
	195B-4R2	- 4078.2	-319.4	15.9	20.7	5.4	-5.7	5.2	-1.3	-0.5
	195B-XYZ	- 3819.4	-507.2	18.3	20.7	2.4	-5.4	1.9	-0.1	-0.3
11/3/77	196A-4	- 4016.3	23.2	-12.2	11.9	6.1	-16.2	5.5	3.6	0.9
	196A-4R1	- 4090.7	1.2	.0	7.8	1.6	-16.1	2.0	2.5	1.8
	196B-4	- 4216.3	32.9	- 3.7	8.5	3.7	-19.0	3.1	4.2	-0.4
	196C-4	- 3821.3	145.1	- 24.4	11.8	6.1	-14.1	5.7	1.4	-1.5
	196C-4R1	- 3765.2	75.6	- 18.3	-14.6	4.1	-41.1	4.3	6.8	-2.5
	196C-4R2	- 3684.7	23.2	- 23.2	12.9	1.2	-11.2	1.2	0.4	-0.4
	196C-XYZ	- 3754.2	-42.7	- 20.7	13.0	2.8	-11.8	3.0	-1.6	-0.8
11/4/77	197A-4	- 3764.9	-20.7	- 13.4	0.3	3.7	-23.4	3.8	2.2	-0.1
	197A-4R1	- 4141.9	69.5	- 11.0	-5.8	1.2	-30.5	0.9	2.1	-0.5
	197A-4R2	- 3941.4	-14.6	- 8.5	7.3	3.1	-20.0	2.7	1.9	0.8
	197A-4R3	- 3595.7	-69.5	-20.7	20.7	0	-7.0	0.2	-1.0	1.2
	197A-5	- 4483.9	3.7	-22.0	7.4	4.2	-18.0	5.0	-3.8	-1.8
	197B-4	- 3643.9	-2.4	- 25.6	-6.6	2.4	-32.0	2.5	3.1	0.2
	197B-4R1	- 3913.3	121.9	- 17.1	7.2	1.7	-17.8	1.6	1.9	0
	197B-4R2	- 4247.7	-20.7	- 30.5	15.4	1.2	-9.4	1.2	-1.6	0.5
	197B-4R3	- 3568.0	-97.5	-22.0	26.7	2.4	-2.9	2.3	-4.0	0.4
	197B-5	- 4623.2	8.5	-30.5	9.1	1.2	-17.7	1.4	-1.2	0.4
MEAN:			21.4	0.6	10.3	3.0	-14.3	2.9	-0.6	-0.4
EST. STANDARD DEVIATION			±214.7	±29.3	±10.4	±1.7	±11.9	± 1.7	±3.9	±1.6

* NOTES:

1. FROM FLIGHT CONTROL COMPUTER - SEE TEXT
2. FROM NAVIGATION COMPUTER - SEE TEXT
3. SAFETY PILOT INTERVENTION - FOR 48 UNAIDED LANDINGS MEANS WERE R = 65.1 ± 59.5 m and Δy = 2.8 ± 2.1 m
4. DATA MISSING DUE TO AUTOPILOT DATA FORMATTER MALFUNCTION
5. DATA NOT AVAILABLE UNTIL AFTER TRANSITION

TABLE I. - CONCLUDED

DECRAB INITIATION (ref. figure 20)		CAT II DECISION HEIGHT (ref. figure 21)		FLARE INITIATION (ref. figure 22)		TOUCHDOWN (ref. figure 23)			REMARKS
Δy, m *1	ΔH, m *1	Δy, m *1	ΔH, m *1	Δy, m *1	ΔH, m *1	Δy, m *1	R_{Rhumb}, m *2	$\dot{h}_{MLS}$, m/sec	
-5.2	-0.2	-2.8 (3)	1.3	-1.7	1.0	-0.4 (3)	179.2 (3)	-0.82	
-5.9	-0.3	-5.5	0.8	-4.9	0.7	-1.4	154.3	-0.52	STAR ABE05
-3.6	0.3	-1.4	1.0	-0.6	1.0	0.7	161.1	-0.73	
-4.1	-0.1	-2.6	1.9	-1.8	1.0	0.5	184.4	-0.76	STAR ABE05
3.7	1.2	5.1	1.8	4.8	1.1	3.0	82.7	-0.88	
-3.6	-1.3	-4.4	1.8	-2.9	1.1	-0.9	116.5	-1.07	STAR ABE05
-0.9	-1.3	0.4	-0.2	0.5	0.2	1.2 (3)	48.8 (3)	-0.73	
-18.0	-1.4	-11.4	0.1	-6.5	0.2	3.4	101.0	-0.64	STAR ABE05
2.4	0.3	3.6	0	3.4	-0.5	2.9	64.2	-1.10	
-0.9	-2.7	2.2	0.8	3.8	0.2	4.6	5.4	-0.76	STAR ABE05
-0.2	1.4	0.2	-0.3	0.8	-0.3	2.1	66.4	-0.73	
2.8	0	2.8	2.2	4.0	0.9	2.4	78.0	-0.92	
-1.2	-2.0	-4.1	-0.9	-1.6	1.0	2.2	96.1	-0.52	
2.2	1.7	2.9	-1.1	2.7	-2.7	1.6	32.3	-0.67	
-1.8	1.3	-0.2	(4)	-0.1	(4)	2.9	98.8	-0.79	
0.9	3.0	0.8	(4)	0.5	1.0	1.9	108.9	-0.95	
1.0	3.0	2.3	2.9	2.3	1.0	4.0	79.8	-1.01	
-2.7	2.6	-1.2	2.1	-0.4	1.2	2.0	160.6	-0.82	
-4.6	-0.9	-5.9	1.9	-4.1	2.1	0.2 (3)	217.7 (3)	-0.43	STAR ABE05
-0.3	2.5	0.3	1.9	0	1.0	2.9	74.5	-1.16	
1.8	-0.1	4.1	0.8	4.3	0.4	4.1	93.8	-1.07	
1.0	1.0	----	----	----	----	----	-----	-----	TRAFFIC ON RUNWAY
-0.8	1.1	0.1	1.2	1.7	0.6	3.4	68.5	-0.85	
-0.1	1.4	1.6	0.9	2.2	0.3	3.0	12.7	-1.04	
-1.8	0.5	0.8	1.2	2.1	0.5	4.4	-14.7	-0.95	STAR ABE05
-4.3	1.1	-2.3	1.6	0.4	0.9	2.8	72.6	-0.82	
-1.3	1.7	-5.0	-2.7	-4.4	-4.0	-4.1	-57.4	-1.01	STAR ABE05
1.1	2.9	1.0	2.7	1.7	1.2	4.1	77.2	-1.16	
0.5	0.4	1.6	-0.3	2.3	0.6	3.0	122.1	-0.73	
1.5	-0.6	5.9	0.5	6.1	0.5	3.9	87.6	-0.89	
2.0	-5.4	5.6	-6.8	5.9	-6.8	6.7	28.4	-0.58	
2.8	2.4	5.0	2.0	4.7	1.6	7.3	58.2	-0.30	
-0.5	-1.2	6.8	-0.5	8.1	-1.2	3.8	6.4	-1.13	
4.7	-2.2	4.4	1.7	2.7	1.0	3.0	221.1	-0.88	
-2.4	-0.9	2.6	-1.6	3.7	-2.2	1.6	11.8	-1.43	
1.3	0.6	0.8	1.1	1.0	0.8	4.7	-16.1	-1.49	
2.9	2.1	2.9	2.7	4.6	1.3	3.9	147.3	-1.10	
2.0	1.1	6.0	-0.4	6.2	2.0	5.5 (3)	-68.4 (3)	-0.98	
4.6	-1.7	7.4	-1.3	7.5	-0.5	4.1	21.6	-1.01	
1.7	-0.2	2.5	1.3	2.8	1.1	2.6	128.8	-0.79	
7.4	-1.2	8.4	-0.6	9.9	-0.9	6.7	11.3	-0.88	
-0.4	1.1	1.5	1.3	2.5	0.1	4.0	-30.5	-0.88	
-0.2	0.1	2.9	-0.1	3.4	-0.2	2.3	52.6	-1.16	
1.5	1.0	1.7	1.3	2.0	1.1	3.2	72.9	-0.79	
3.0	1.2	3.6	2.3	5.3	2.8	4.3	43.7	-0.76	
1.7	1.5	2.4	1.6	3.6	0.6	3.5	8.6	-0.76	
-0.3	1.3	0	1.1	0.3	1.1	0.7	86.5	-0.85	
-2.4	0	0.8	0.7	1.0	0.5	3.0	-37.7	-1.01	STAR ABE05
4.3	0.2	6.0	-0.8	5.5	-2.0	5.2	14.8	-0.95	
2.8	-0.1	3.8	-0.5	4.0	-0.4	2.2	61.6	-0.92	
0.8	0.2	4.0	0.5	-0.7	0.3	-1.1	39.6	-0.76	
-3.4	1.4	-0.3	0.4	1.7	0.3	1.3	44.3	-0.64	
-0.5	2.0	2.3	1.7	3.1	1.0	2.2	22.8	-1.07	STAR ABE05
-0.2	0.4	1.4	0.6	2.0	0.3	2.7	67.4	-0.88	
±3.7	±1.6	±3.8	±1.6	±3.3	±1.6	±2.1	±65.8	±0.22	

TABLE II. - SUMMARY OF WIND VS. ALTITUDE

Altitude, MSL, m (ft)	North Velocity, knots	East Velocity, knots	Resultant Wind, deg. mag., knots
305 (1000)	-4.37 ± 8.45	9.27 ± 12.66	115, 10.3
152 (500)	-1.61 ± 6.65	8.79 ± 9.41	100, 8.9
91 (300)	-2.49 ± 6.37	8.44 ± 9.28	106, 8.8
61 (200)	-2.63 ± 5.53	7.92 ± 8.65	108, 8.3
30 (100)	-3.64 ± 4.02	5.13 ± 5.50	125, 6.3
15 (50)	-3.44 ± 3.35	3.82 ± 5.43	132, 5.1

NOTE: Runway Heading is 127°

TABLE III. - COMPARISON OF BAROMETRIC AND TRSB-DERIVED VERTICAL SPEEDS

LOCATION	FILTERED BARO VERTICAL SPEED $\dot{h}_{CF}$, m/sec	TRSB-DERIVED VERTICAL SPEED $\dot{h}_{MLS}$, m/sec	$\dot{h}_{CF} - \dot{h}_{MLS}$, m/sec
FAF3K	-3.80 ± 0.45	-3.81 ± 0.48	0.01
FAF2K	-3.42 ± 0.19	-3.63 ± 0.23	0.21
CAT I DH	-2.91 ± 0.41	-3.06 ± 0.42	0.15
DECRAB	-3.02 ± 0.33	-3.14 ± 0.35	0.12
CAT II DH	-3.40 ± 0.34	-3.45 ± 0.39	0.04
FLARE	-3.43 ± 0.36	-3.40 ± 0.41	-0.03
TOUCHDOWN	-1.28 ± 0.24	-0.88 ± 0.22	-0.39

TABLE IV. - COMPARISON OF INDICATED ALTITUDE ERRORS (1)

LOCATION	ERROR IN IDDALT, m (BARO ALT.)(2)	ERROR IN h_{MLS}, m (TRSB ALT.)(3)	ERROR IN h_R, m (RADIO ALT.)(4)
FAF	16.76 ± 23.59	2.80 ± 3.38	7.56 ± 7.92
CAT I DH	12.80 ± 21.52	-1.04 ± 1.89	4.48 ± 4.82
CAT II DH	12.62 ± 21.15	0.03 ± 1.68	0.70 ± 1.98
TOUCHDOWN	9.57 ± 20.30	0.37 ± 0.49	0.46 ± 0.70

NOTES:

1. And standard deviation.
2. IDDALT is the altitude of the aircraft static pressure ports, which was assumed to be approximately the same as the center of gravity.
3. h_{MLS} is the altitude of the aircraft center of gravity, which was taken to be 3.0 m (9.8 ft) above the GPIP elevation at touchdown.
4. Radio altimeters are calibrated to read wheel height in nominal landing attitude. Measured altitude was corrected for a 2.7^{o} mean pitch attitude difference between landing and approach configurations, and an assumed ground elevation of 5.18 m (17 ft) (the elevation of the GPIP). The latter correction was not made at waypoint FAF3K, which was over the river so that radio altitude was equal to altitude MSL.

Figure 1. - NASA TCV B-737 Research Aircraft.

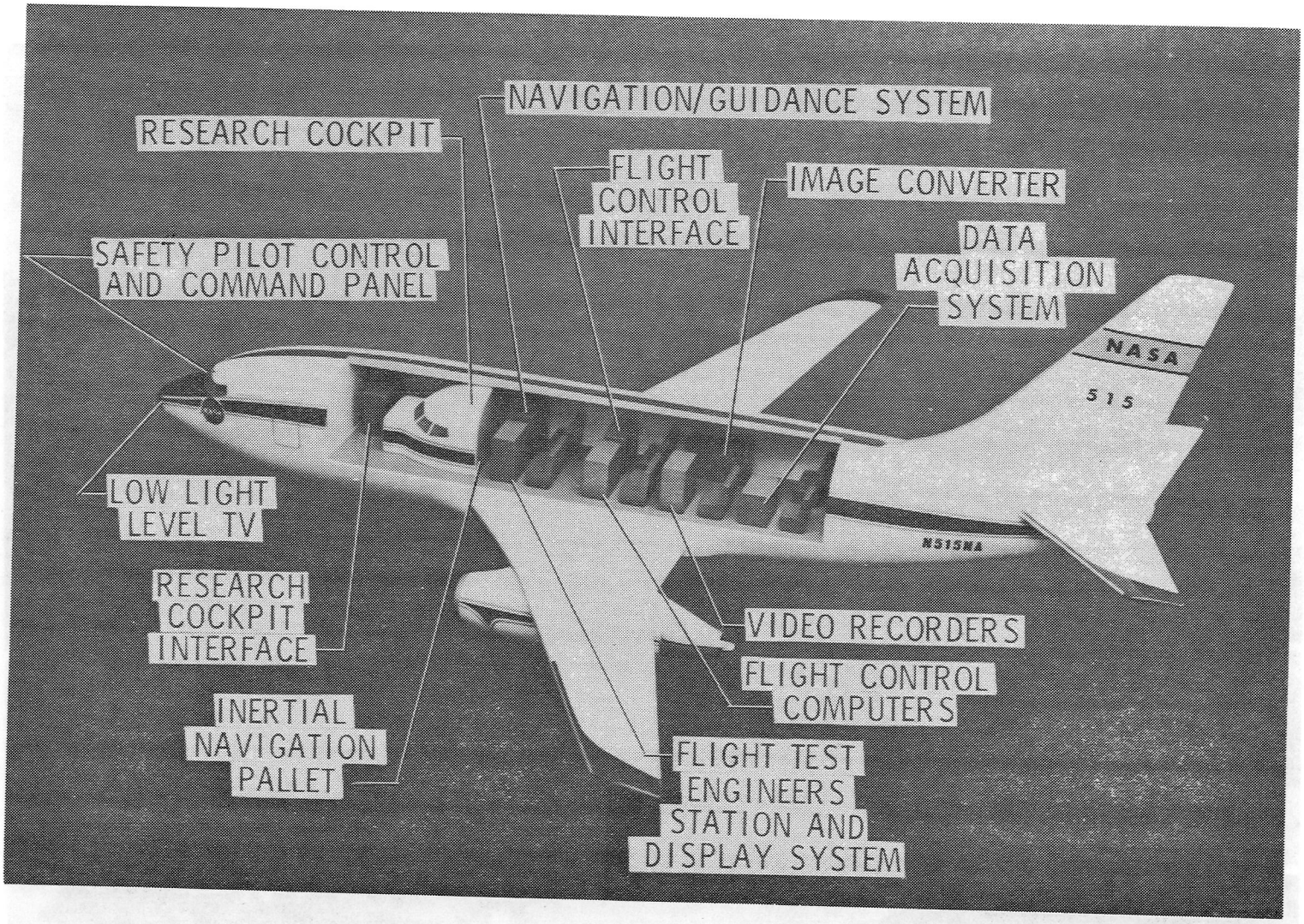

Figure 2. - NASA TCV B-737 Research Aircraft (Internal Arrangement).

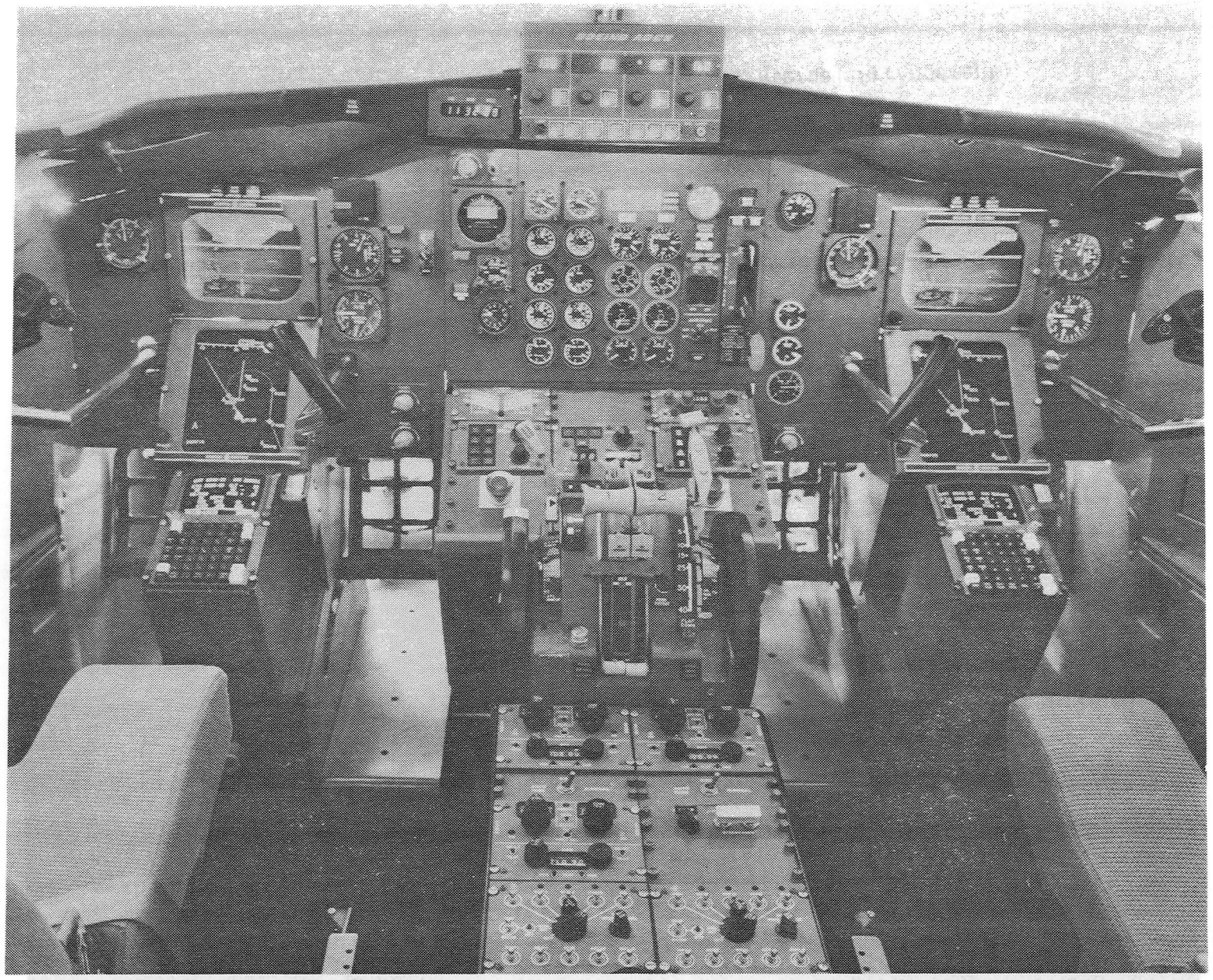

Figure 3. - Aft Flight Deck Display Arrangement.

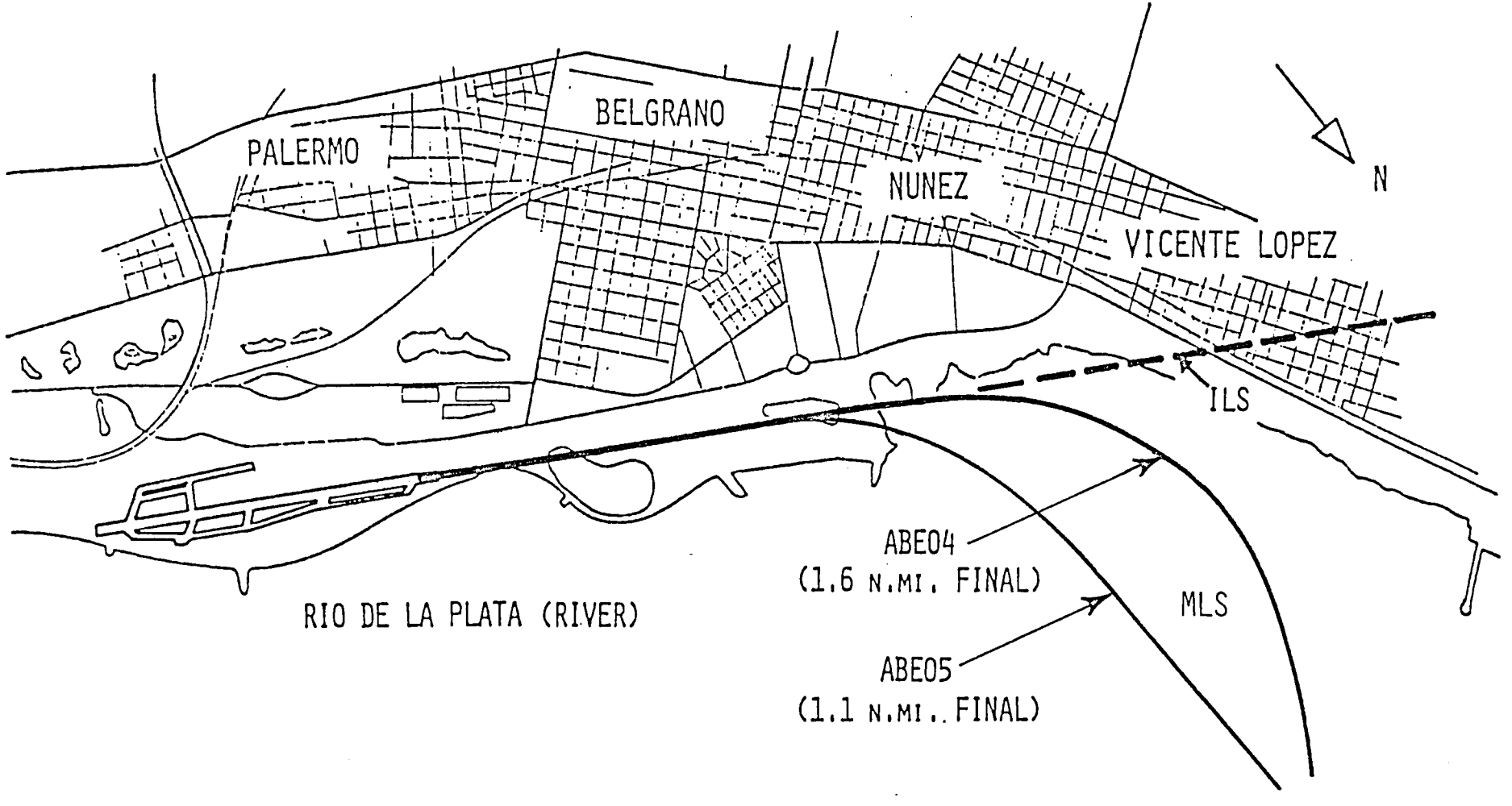

Figure 4. - Approach Paths for Automatic MLS Landings by TCV B-737 at Jorge Newbery Airport, Buenos Aires, Argentina.

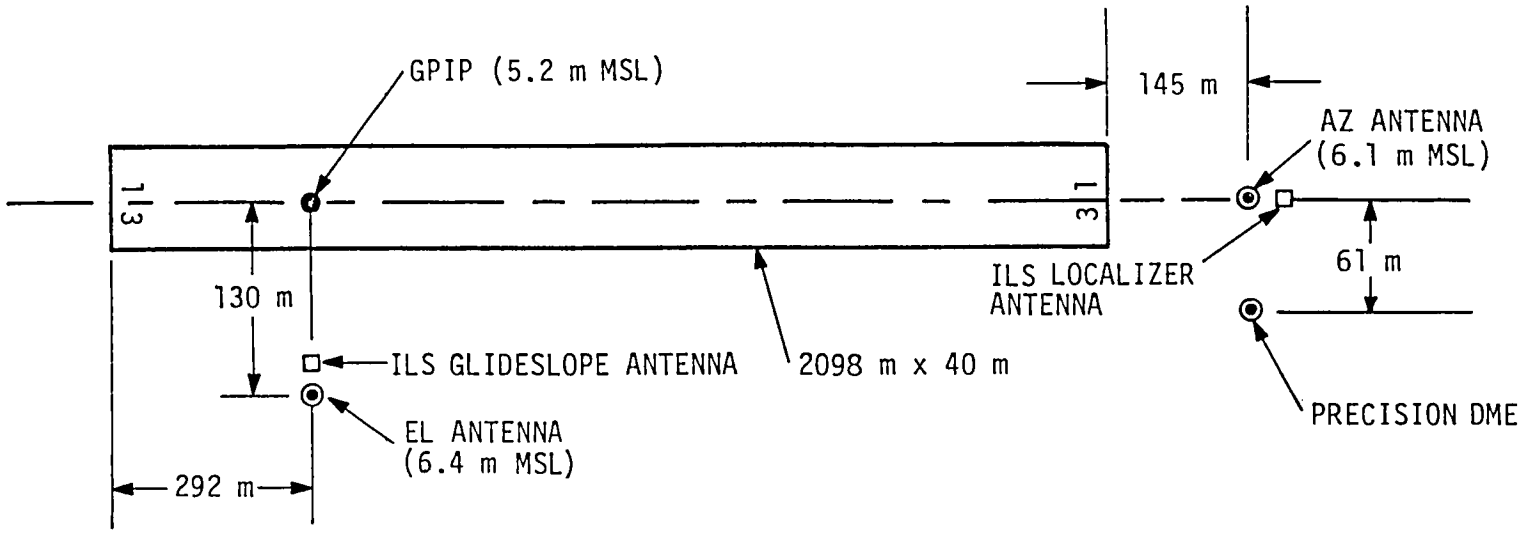

RUNWAY TRUE HEADING: 124.2°

AZ ANTENNA COORDINATES: 34°33'59" S, 58°24'17" W

GPIP COORDINATES: 34°33'23" S, 58°25'20" W

NOTE: DRAWING NOT TO SCALE

Figure 5. - MLS Configuration for Runway 13 at Jorge Newbery Airport.

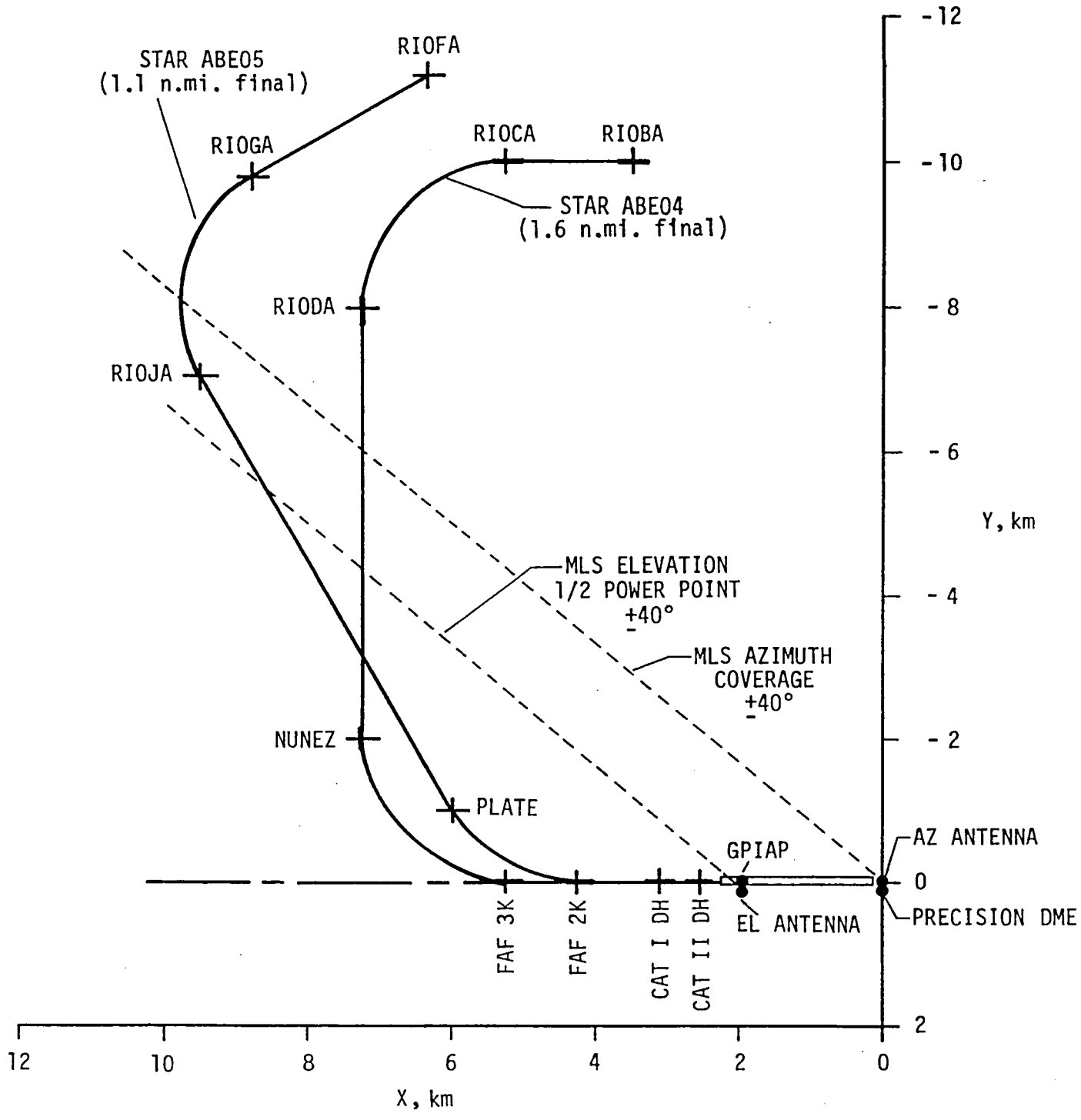

Figure 6. - Standard Terminal Arrival Routes used by TCV B-737 for Automatic MLS Approaches to Jorge Newbery Airport.

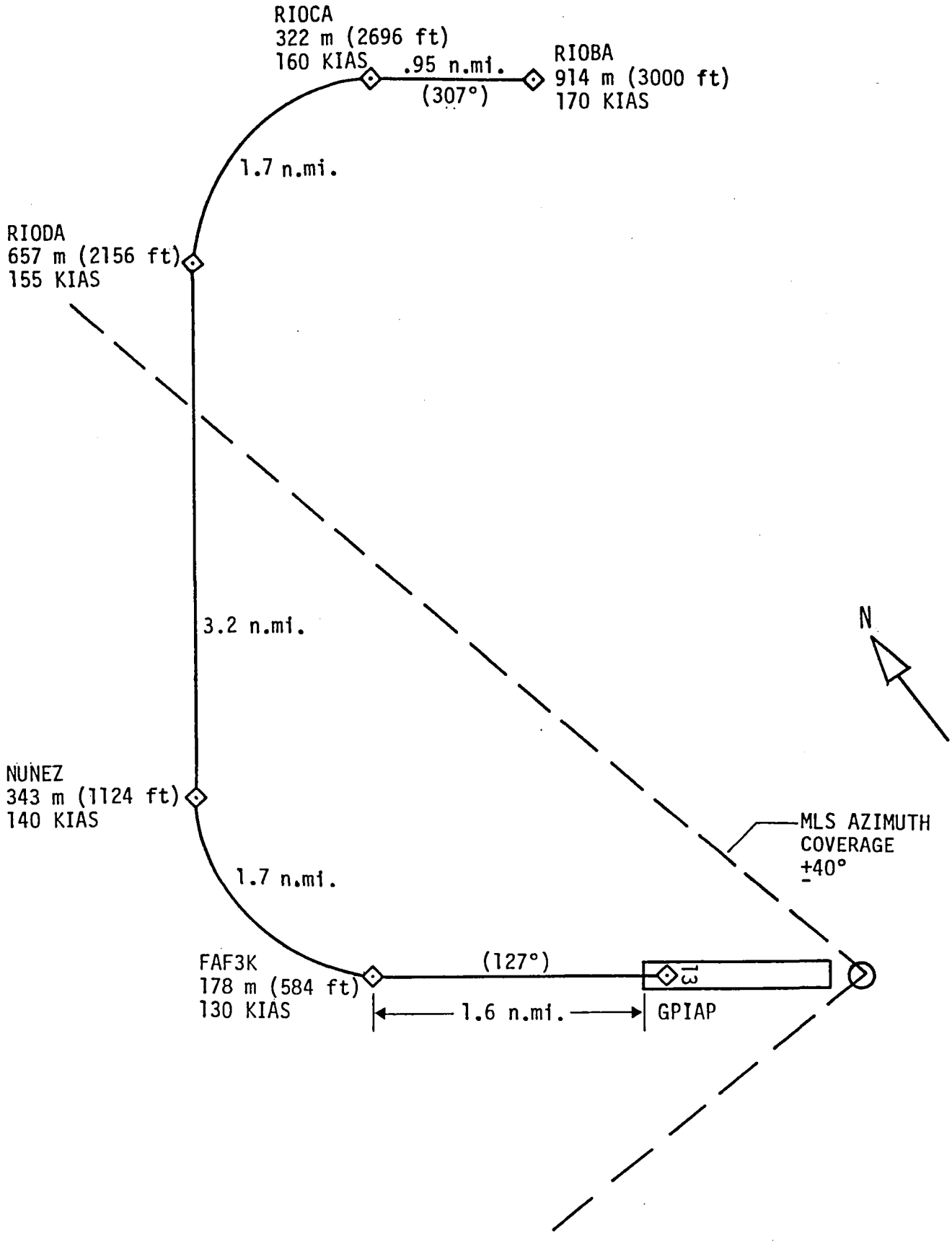

Figure 7. - Standard Terminal Arrival Route ABE04 to Jorge Newbery Airport.

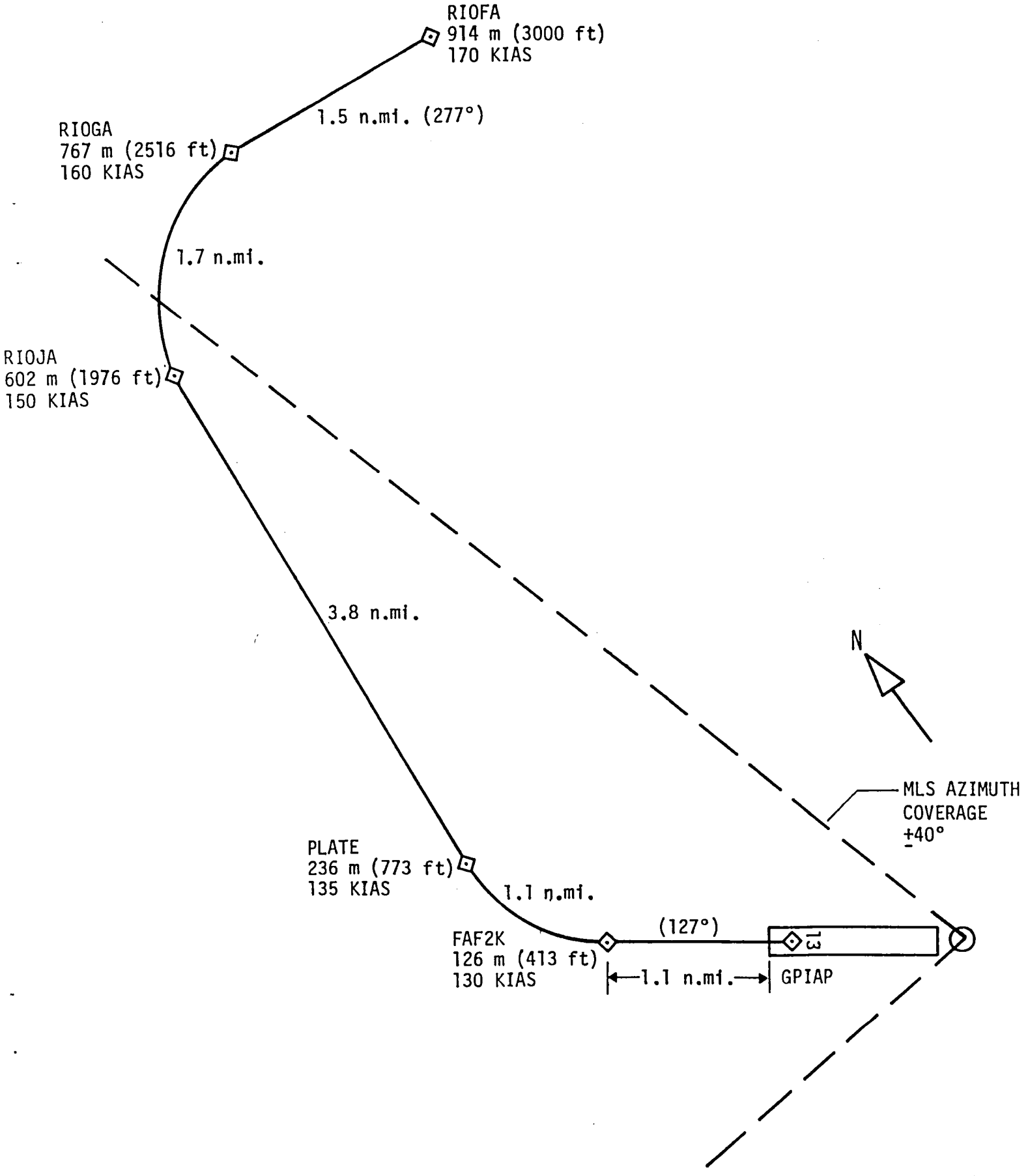

Figure 8. - Standard Terminal Arrival Route ABE05 to Jorge Newbery Airport.

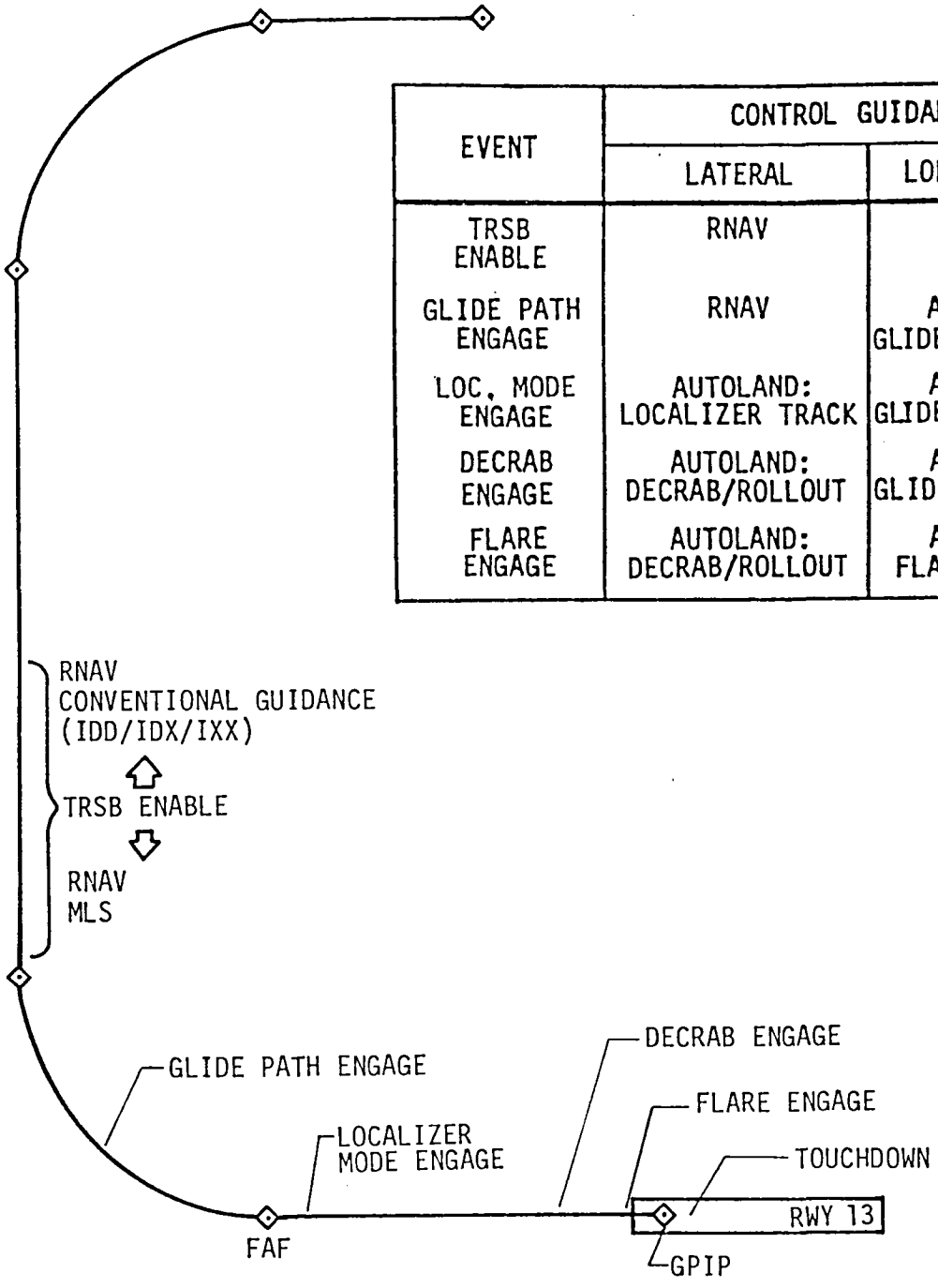

EVENT	CONTROL GUIDANCE	
	LATERAL	LONGITUDINAL
TRSB ENABLE	RNAV	RNAV
GLIDE PATH ENGAGE	RNAV	AUTOLAND: GLIDE PATH TRACK
LOC. MODE ENGAGE	AUTOLAND: LOCALIZER TRACK	AUTOLAND: GLIDE PATH TRACK
DECRAB ENGAGE	AUTOLAND: DECRAB/ROLLOUT	AUTOLAND: GLIDE PATH TRACK
FLARE ENGAGE	AUTOLAND: DECRAB/ROLLOUT	AUTOLAND: FLARE/ROLLOUT

Figure 9. - TCV B737 Control Law Schedule for Jorge Newbery Automatic MLS Approaches and Landings.

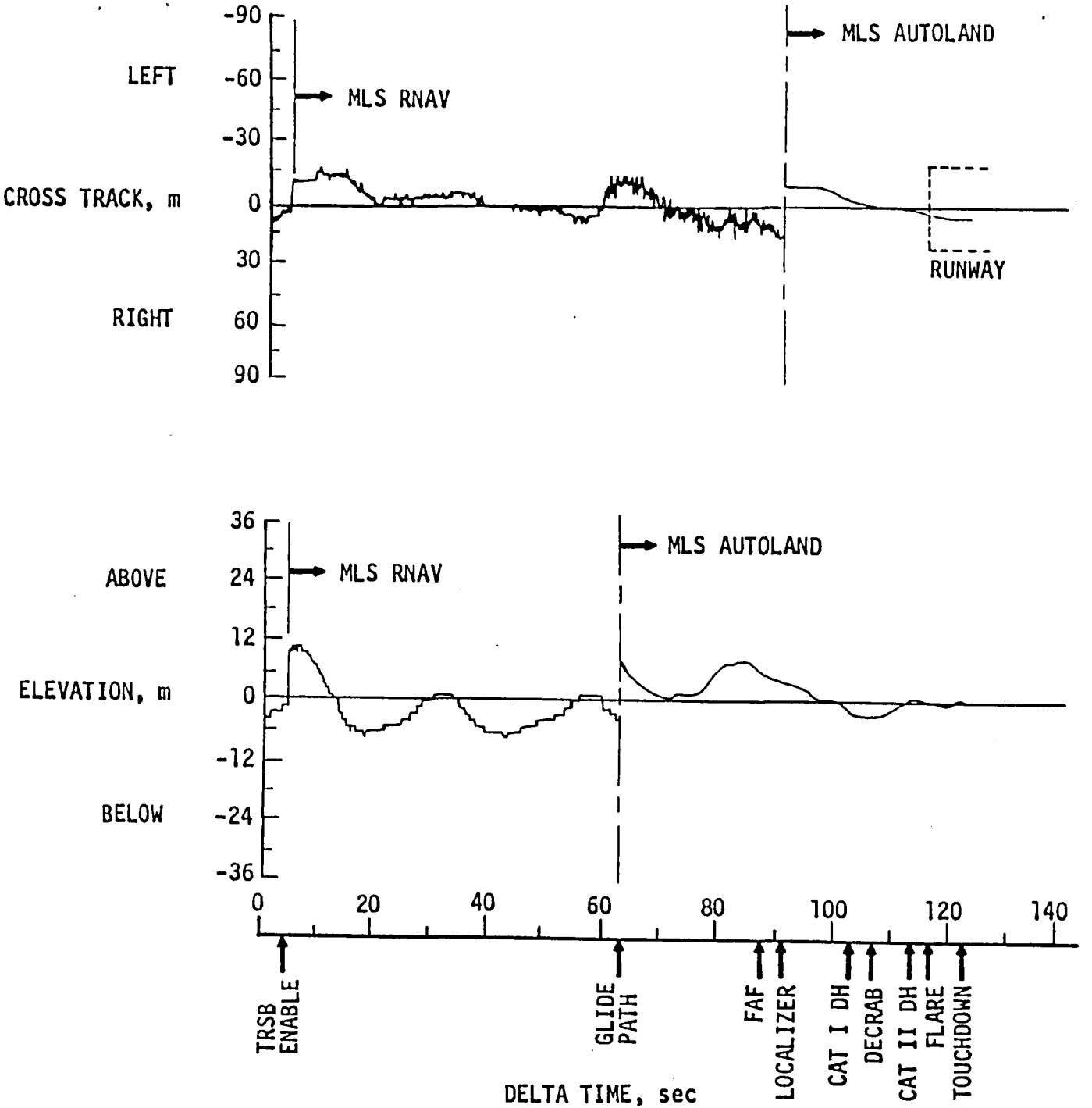

Figure 10. - Flight Technical Errors for Typical Automatic MLS Approach at Jorge Newbery (Flight/Run No. 192 - 4R1).

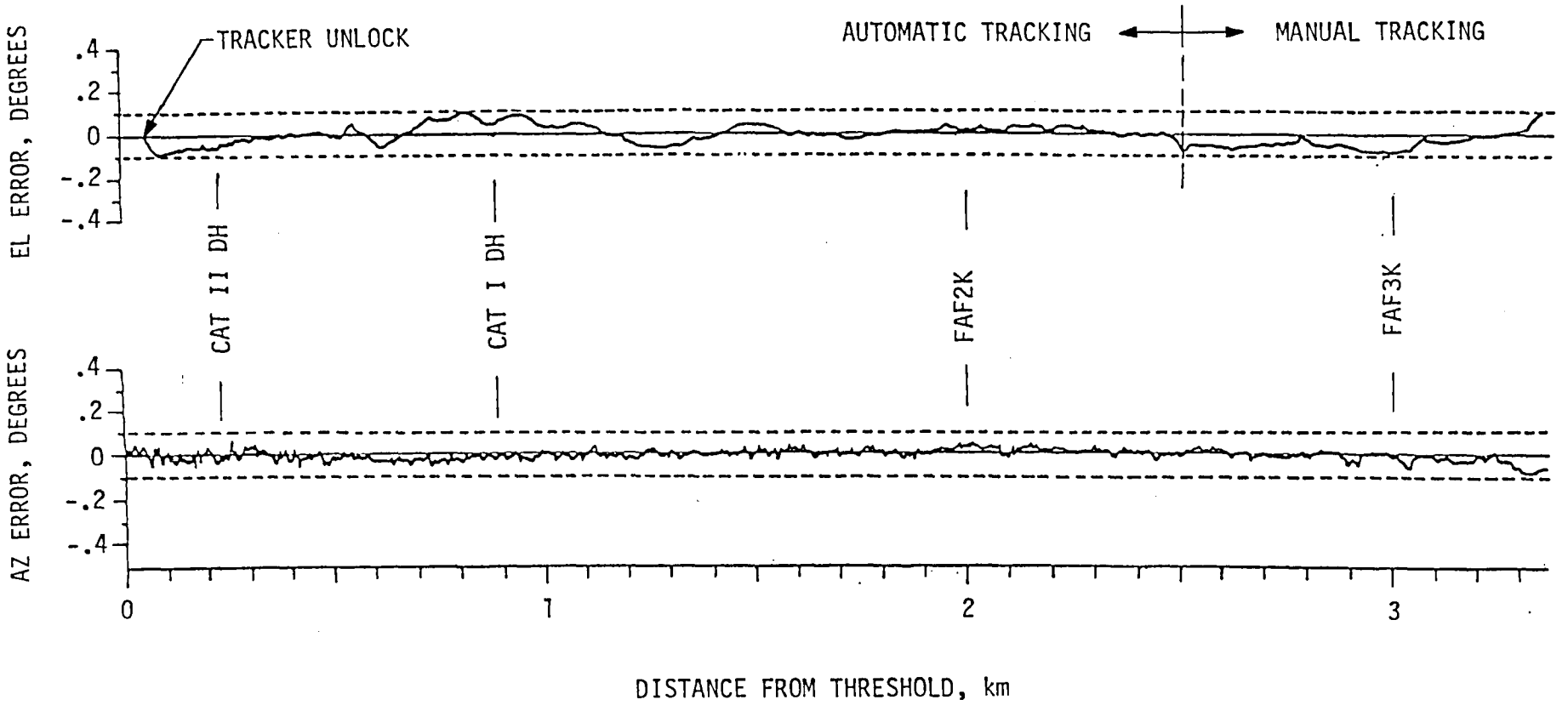

Figure 11. - Example of TRSB Angle Errors Derived from Ground Tracking Data.

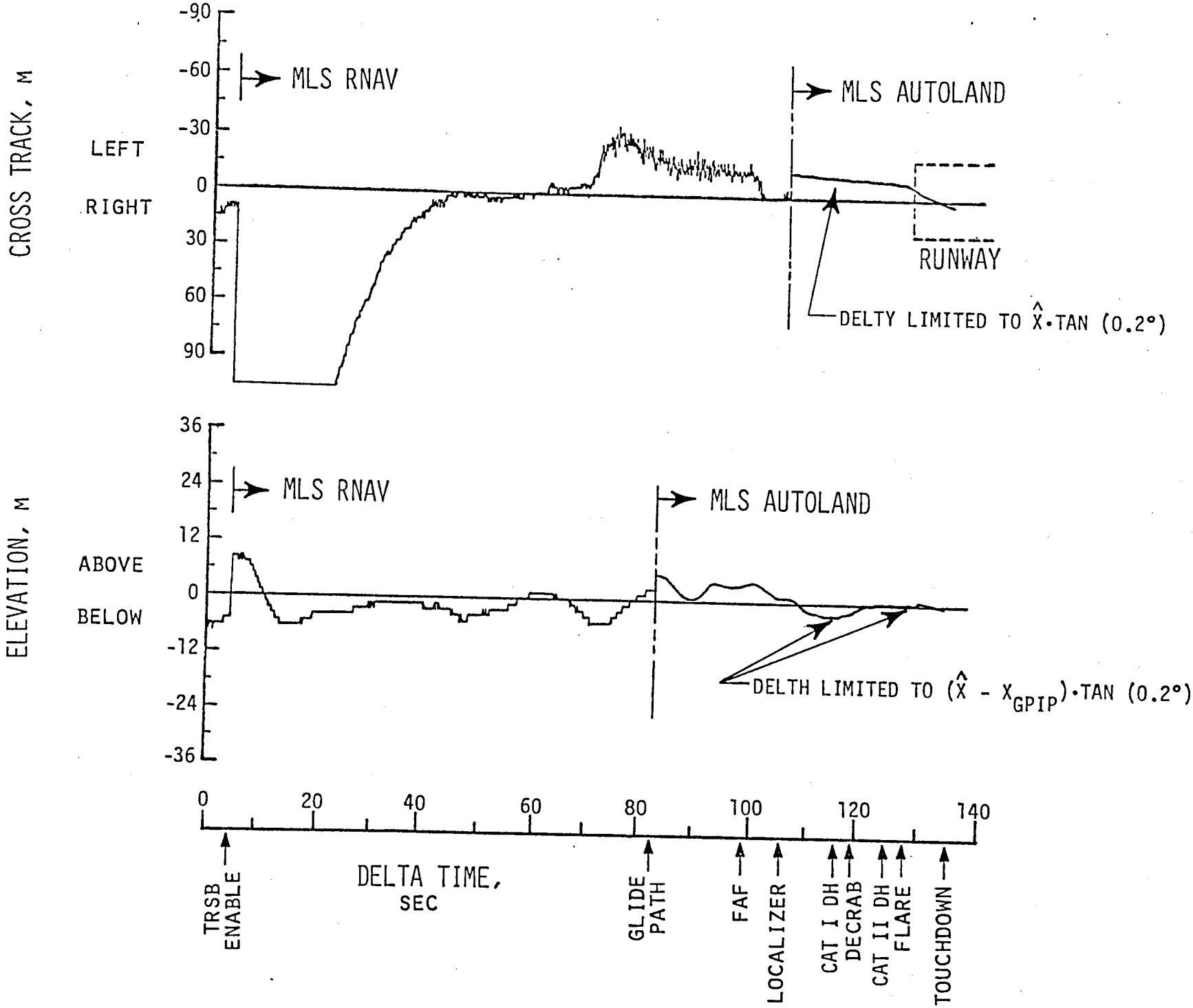

Figure 12. - Illustration of Limited Guidance Error Signals in Autoland Mode (Flight/Run No. 192-4).

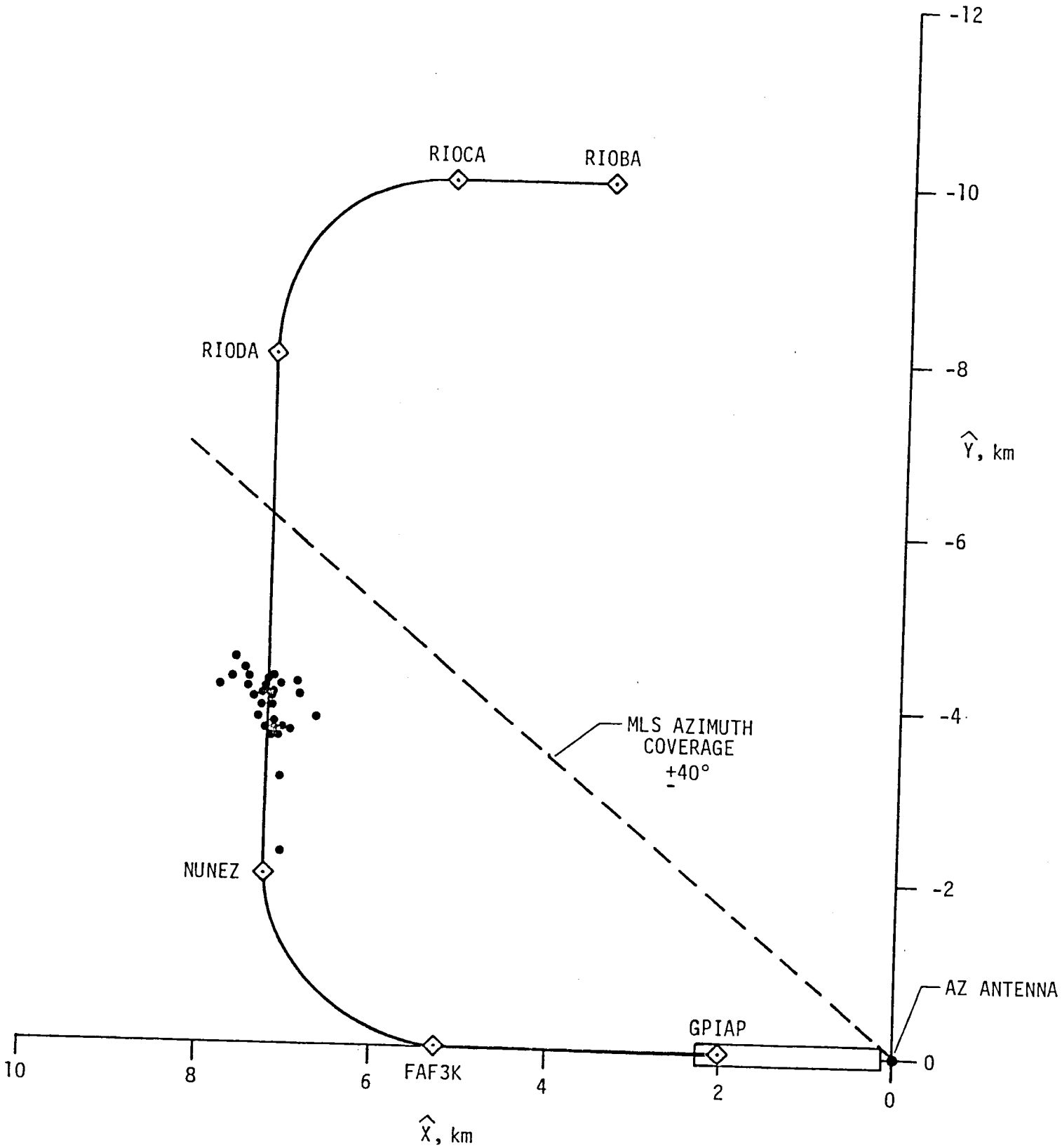

Figure 13. - Summary of Conventional-to-MLS RNAV Lateral Path Offsets for TCV B-737 Automatic MLS Approaches to Jorge Newbery on STAR ABE04.

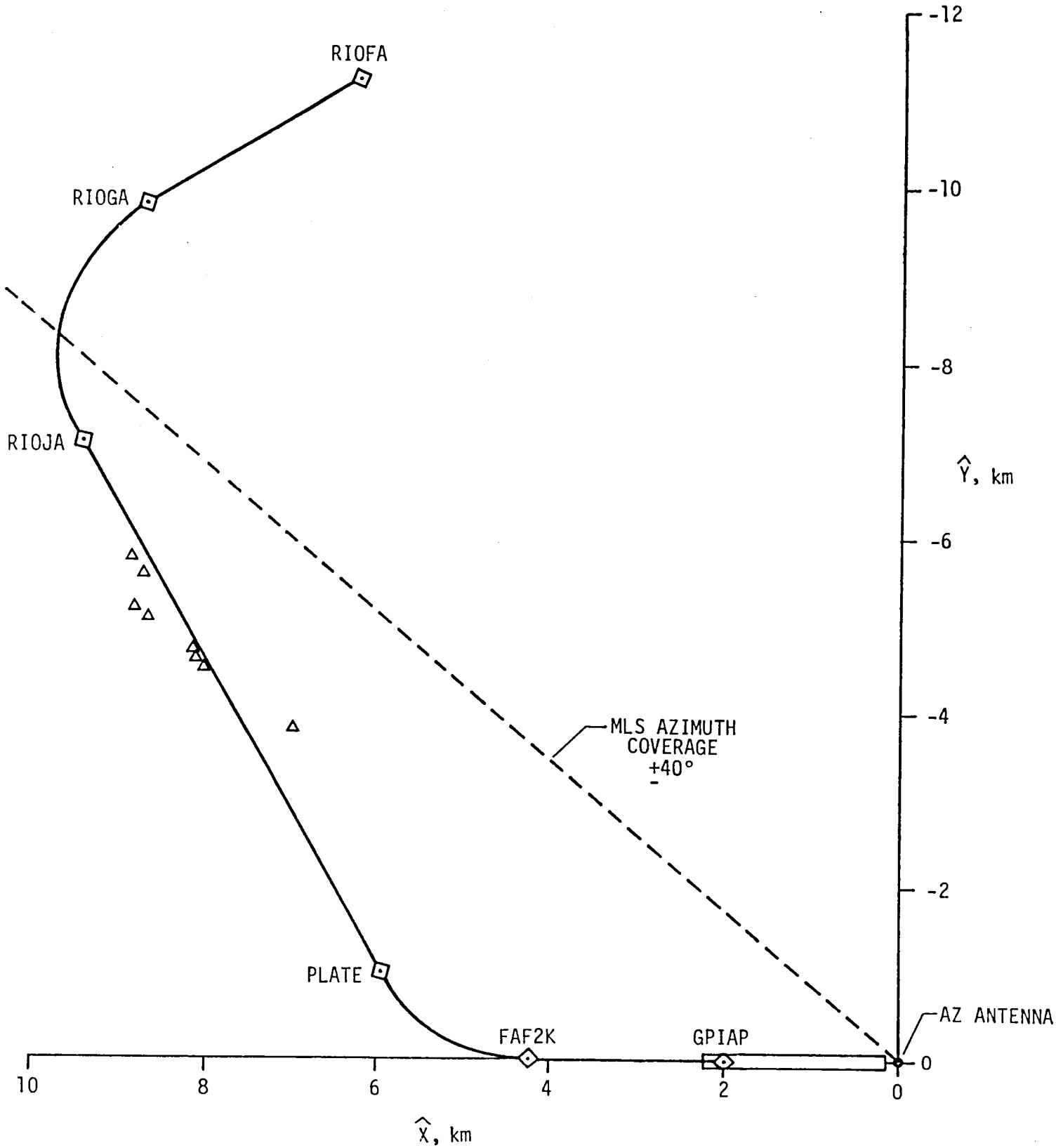

Figure 14.- Summary of Conventional-to-MLS RNAV Lateral Path Offsets for TCV B-727 Automatic MLS Approaches to Jorge Newbery on STAR ABE05.

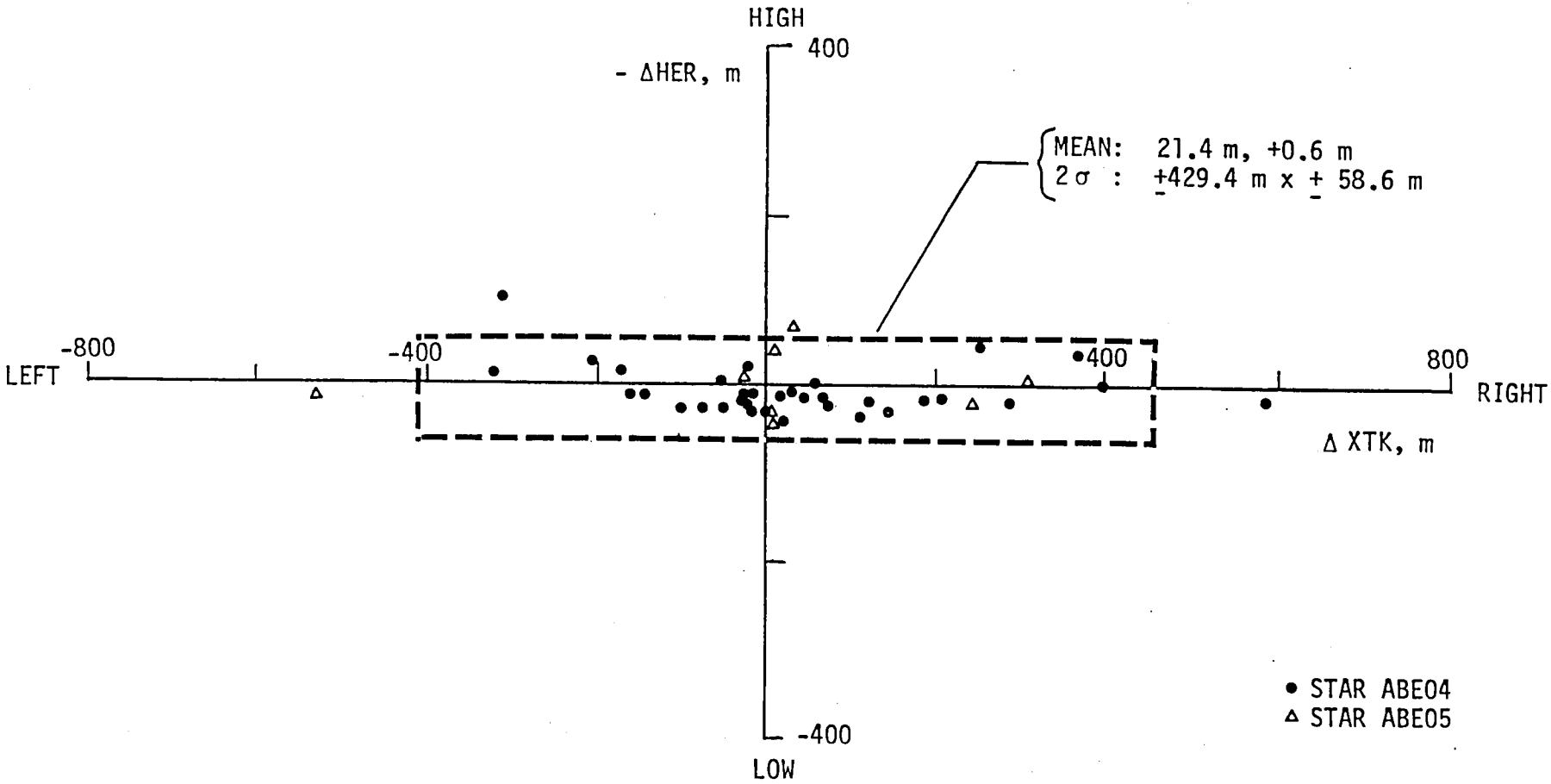

Figure 15. - Summary of - ΔHER versus ΔXTK at Conventional-to-MLS RNAV Transition for Jorge Newbery Automatic MLS Approaches.

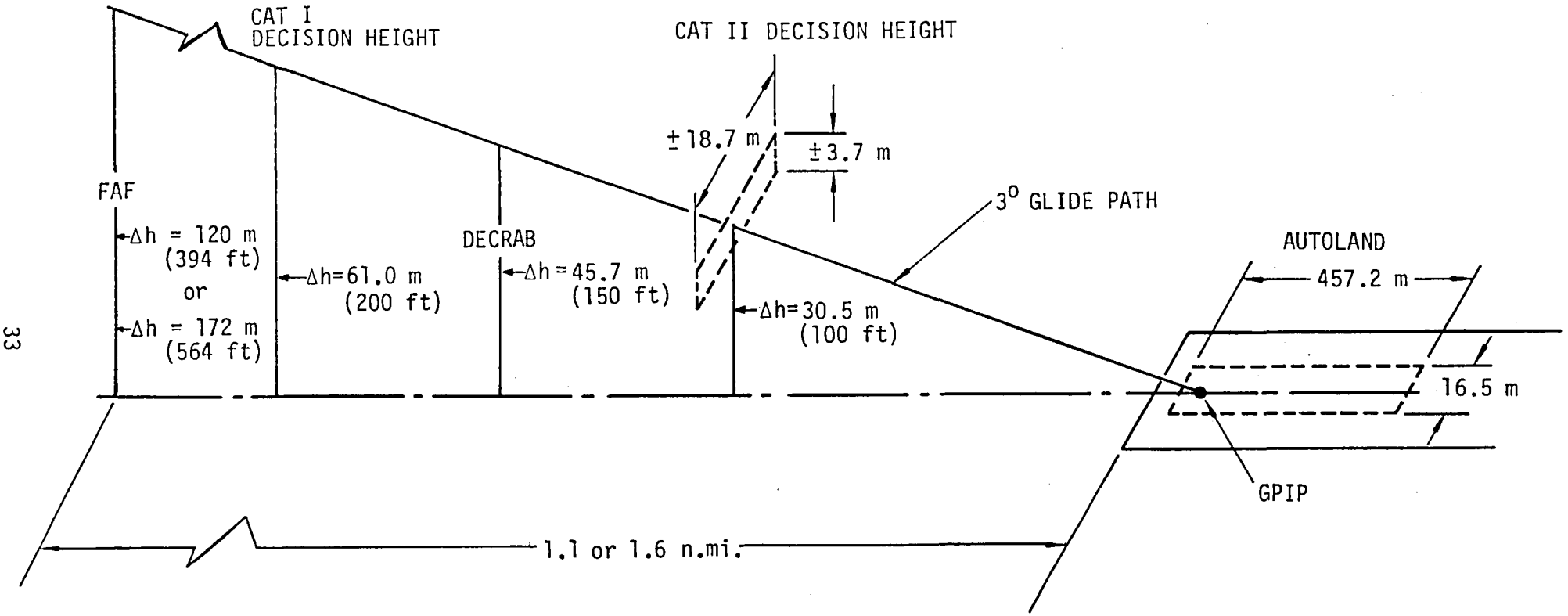

Figure 16. - Jorge Newbery Approach and Landing Profile Including FAA Certification Criteria (2 σ).

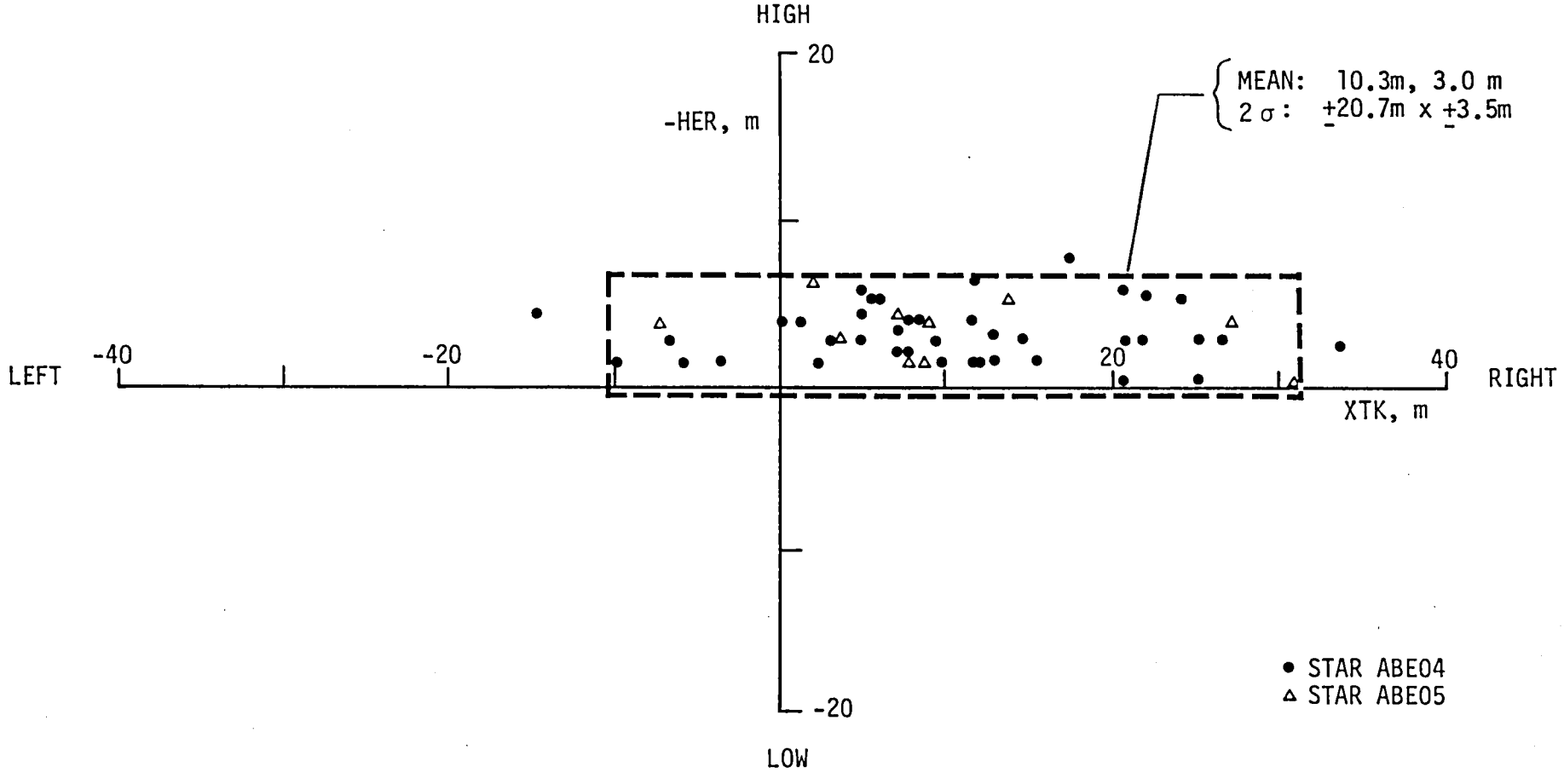

Figure 17. - Summary of - HER versus XTK at the Final Approach Fix for Jorge Newbery Automatic MLS Approaches.

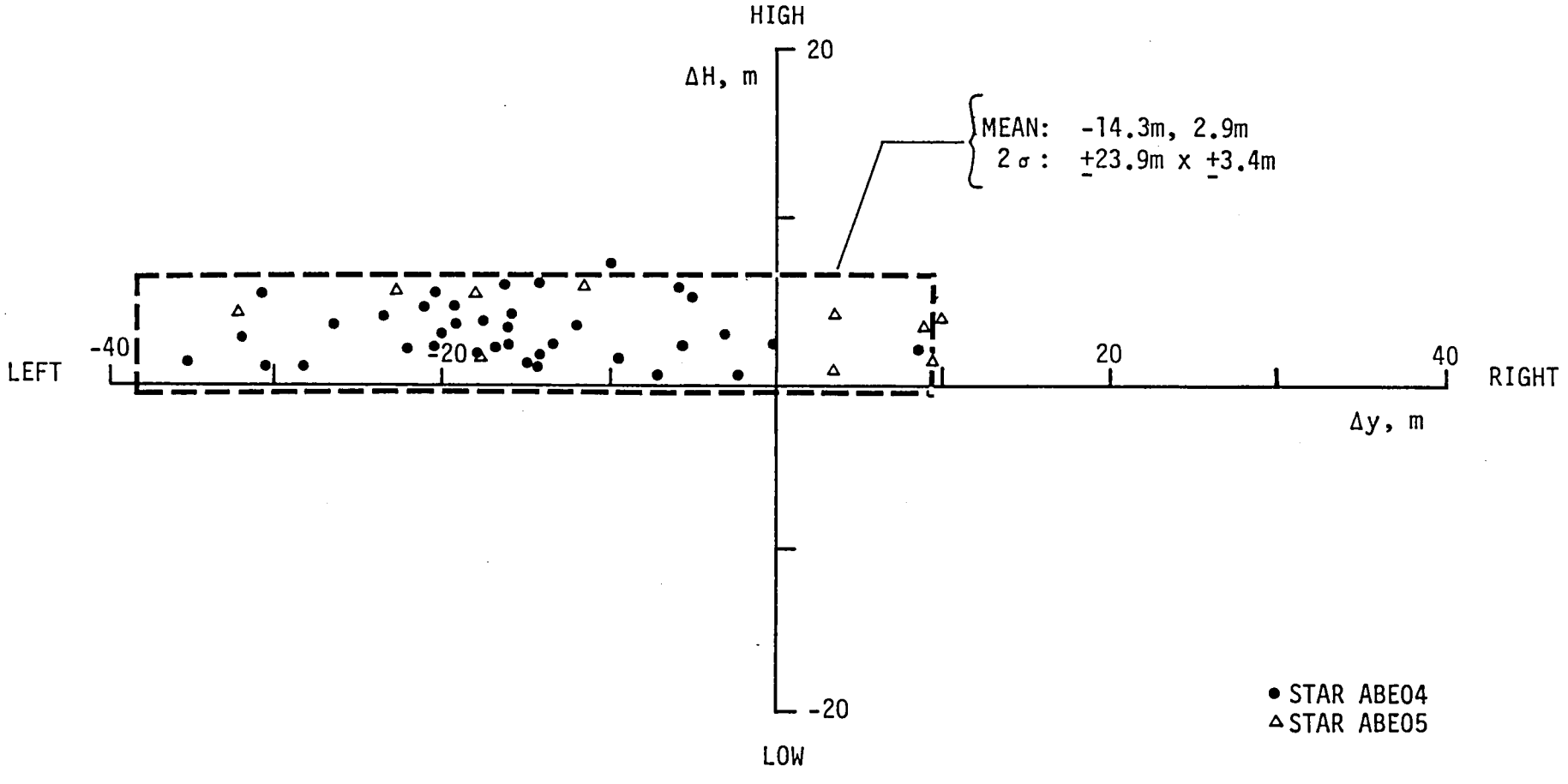

Figure 18. - Summary of TRSB - Derived Errors at the Final Approach Fix for Jorge Newbery Automatic MLS Approaches.

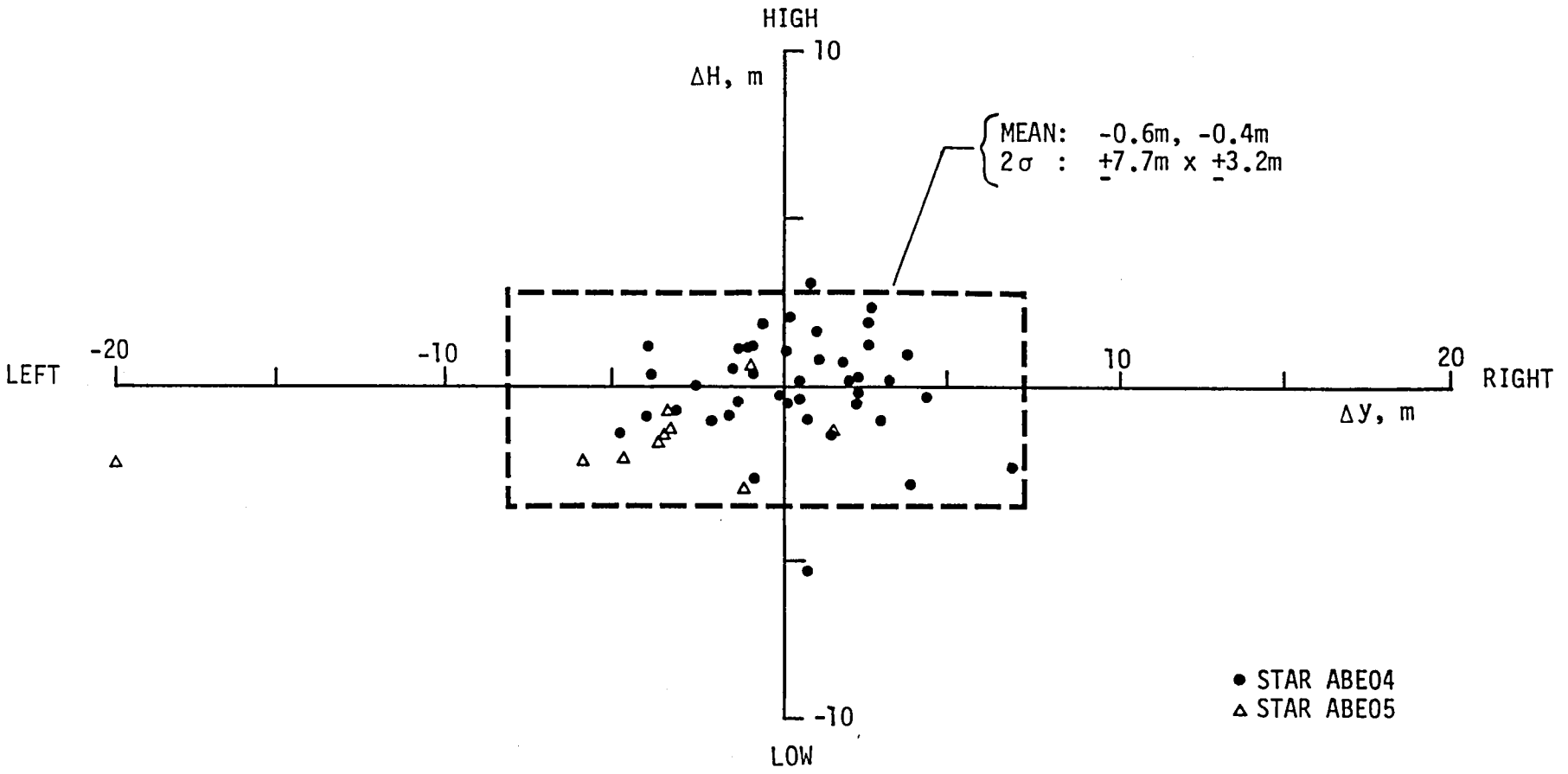

Figure 19. - Summary of TRSB - Derived Errors at the CAT I Decision Height for Jorge Newbery Automatic MLS Approaches.

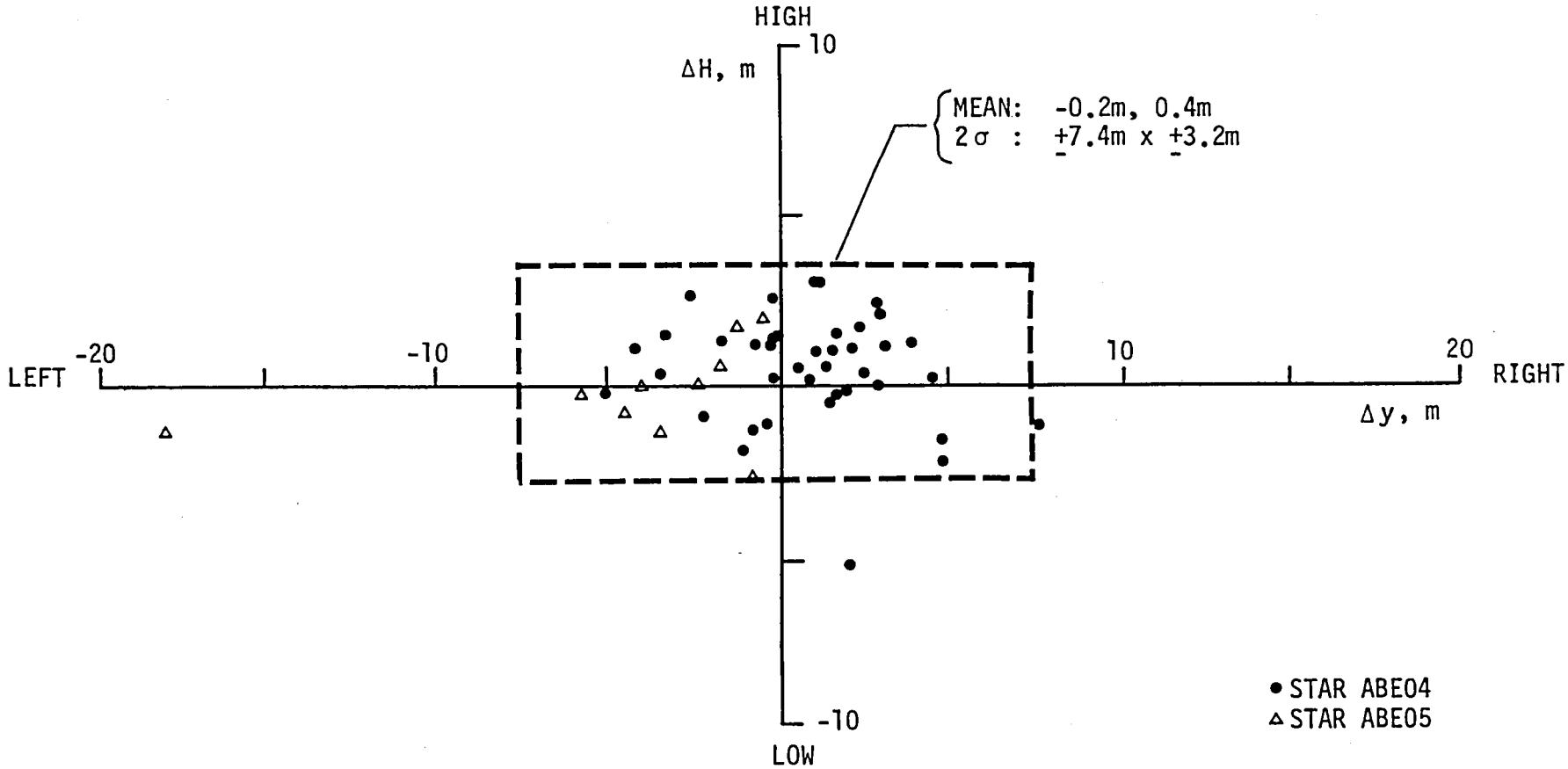

Figure 20. - Summary of TRSB - Derived Errors at Decrab Initiation for Jorge Newbery Automatic MLS Approaches.

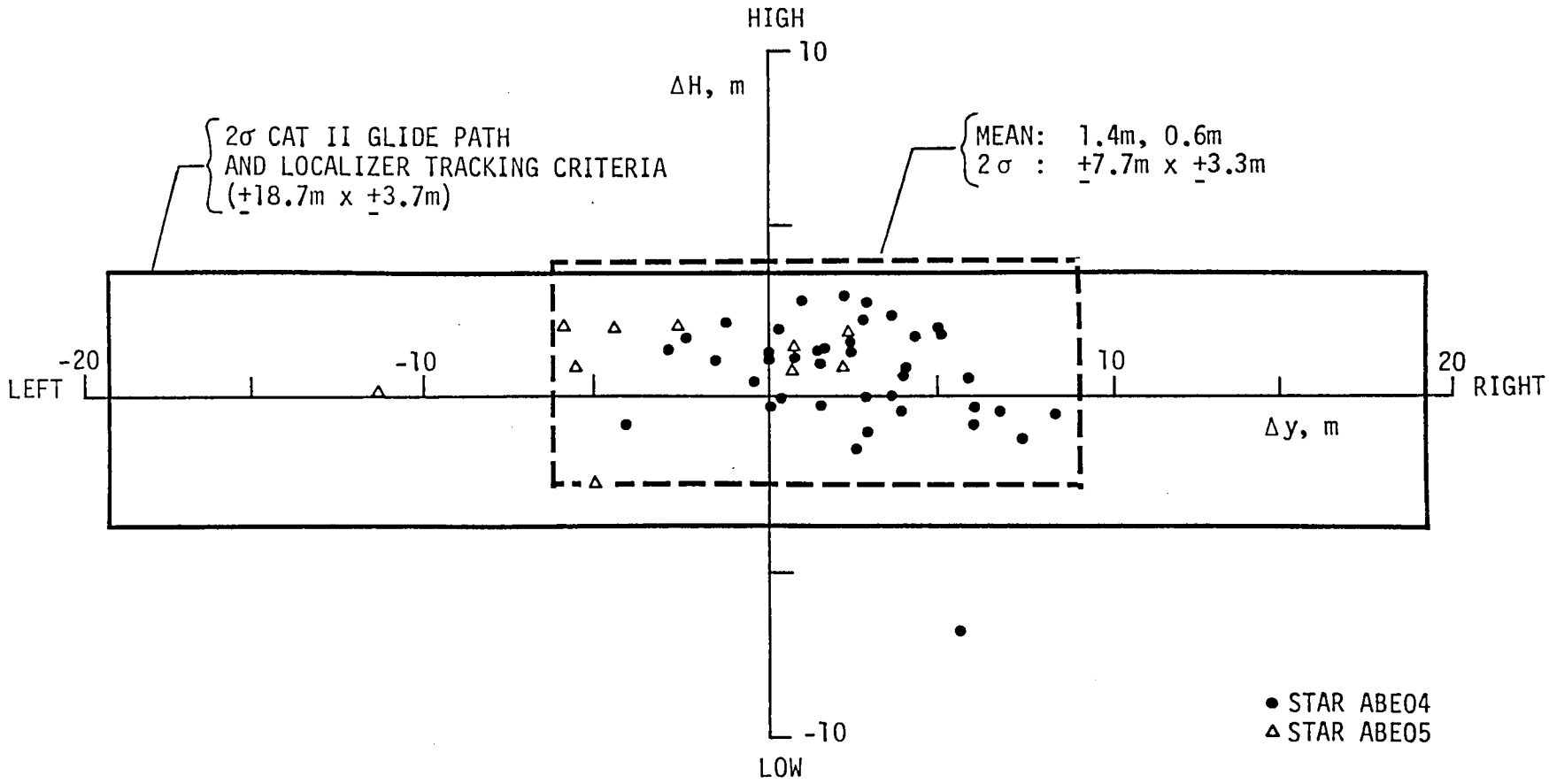

Figure 21. - Summary of TRSB - Derived Errors at the CAT II Decision Height for Jorge Newbery Automatic MLS Approaches.

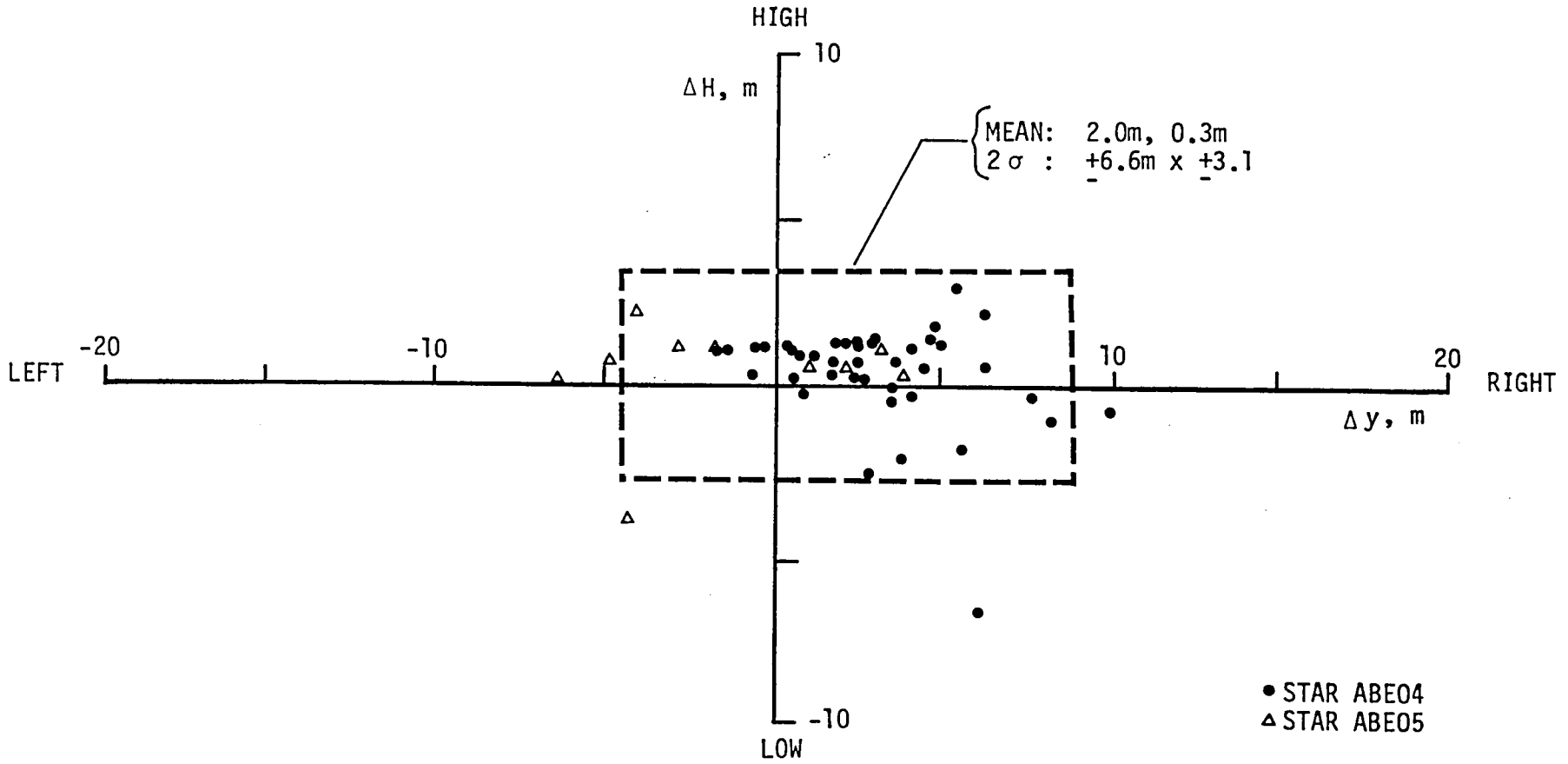

Figure 22. - Summary of TRSB - Derived Errors at Flare Initiation for Jorge Newbery Automatic MLS Landings.

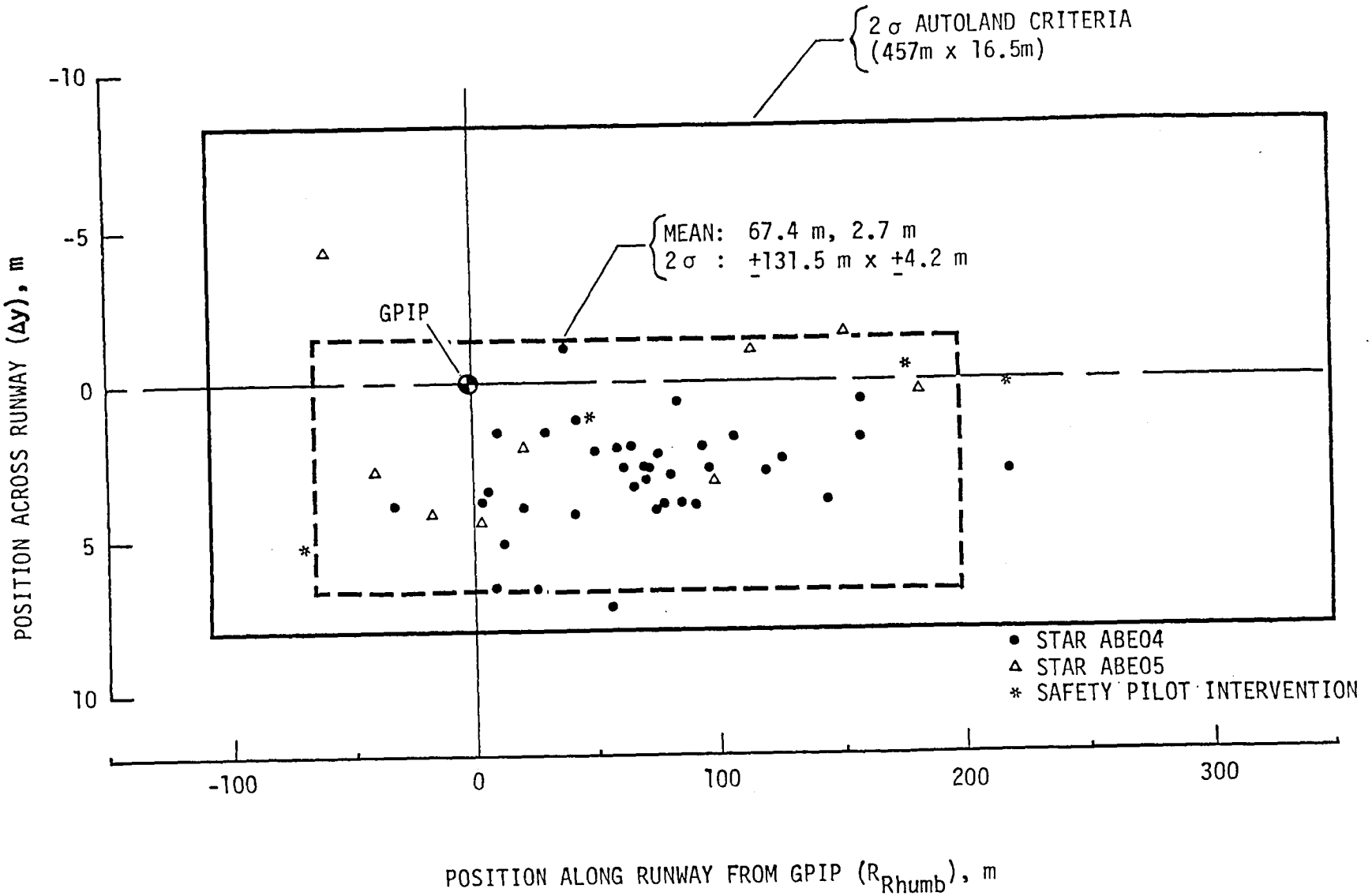

Figure 23. - Summary of TRSB - Derived Touchdown Performance of TCV B-737 for Jorge Newbery Automatic MLS Landings.

1. Report No.	2. Government Accession No.	3. Recipient's Catalog No.
NASA TM-80223		

4. Title and Subtitle	5. Report Date
FLIGHT PERFORMANCE OF THE TCV B-737 AIRPLANE AT JORGE NEWBERY AIRPORT, BUENOS AIRES, ARGENTINA USING TRSB/MLS GUIDANCE	January 1980
	6. Performing Organization Code
7. Author(s)	8. Performing Organization Report No.
William F. White and Leonard V. Clark	
9. Performing Organization Name and Address	10. Work Unit No.
NASA Langley Research Center Hampton, VA 23665	534-04-13-62
	11. Contract or Grant No.
12. Sponsoring Agency Name and Address	13. Type of Report and Period Covered
National Aeronautics and Space Administration Washington, DC 20546	Technical Memorandum
	14. Sponsoring Agency Code

15. Supplementary Notes

16. Abstract

The NASA Terminal Configured Vehicle B-737 was flown at Jorge Newbery Airport, Buenos Aires, Argentina in support of the world-wide FAA demonstration of the Time Reference Scanning Beam/Microwave Landing System. This report presents a summary of the flight performance of the TCV airplane during demonstration automatic approaches and landings while utilizing TRSB/MLS guidance. The TRSB/MLS was shown to provide the terminal area guidance necessary for flying curved automatic approaches with final legs as short as 2 km (1.1 n.mi.).

17. Key Words (Suggested by Author(s))	18. Distribution Statement
Microwave Landing System Time Reference Scanning Beam Landing Guidance Systems Automatic Landings Curved Approaches	Unclassified - Unlimited Subject Category 04

19. Security Classif. (of this report)	20. Security Classif. (of this page)	21. No. of Pages	22. Price*
Unclassified	Unclassified	40	$4.50

For sale by the National Technical Information Service, Springfield, Virginia 22161